



Natural and Anthropogenic Geohazards in Greater London Observed from Geological and ERS-1/2 and ENVISAT Persistent Scatterers Ground Motion Data: Results from the EC FP7-SPACE PanGeo Project

FRANCESCA CIGNA,¹ HANNAH JORDAN,¹ LUKE BATESON,¹ HARRY MCCORMACK,² and CLAIRE ROBERTS²

Abstract—We combine geological data and ground motion estimates from satellite ERS-1/2 and ENVISAT persistent scatterer interferometry (PSI) to delineate areas of observed natural and anthropogenic geohazards in the administrative area of Greater London (United Kingdom). This analysis was performed within the framework of the EC FP7-SPACE PanGeo project, and by conforming to the interpretation and geohazard mapping methodology extensively described in the Production Manual (cf. <http://www.pangeoproject.eu>). We discuss the results of the generation of the PanGeo digital geohazard mapping product for Greater London, and analyse the potential of PSI, geological data and the PanGeo methodology to identify areas of observed geohazards. Based on the analysis of PSI ground motion data sets for the years 1992–2000 and 2002–2010 and geology field campaigns, we identify 25 geohazard polygons, covering a total of ~ 650 km². These include not only natural processes such as compaction of deposits on the River Thames flood plain and slope instability, but also anthropogenic instability due to groundwater management and changes in the Chalk aquifer, recent engineering works such as those for the Jubilee Line Extension project and electricity tunnelling in proximity to the River Thames, and the presence of made ground. In many instances, natural and anthropogenic observed geohazards overlap, therefore indicating interaction of different processes over the same areas. In terms of ground area covered, the dominant geohazard is anthropogenic land subsidence caused by groundwater abstraction for a total of ~ 300 km², followed by natural compression of River Thames sediments over ~ 105 km². Observed ground motions along the satellite line-of-sight are as high as +29.5 and -25.3 mm/year, and indicate a combination of land surface processes comprising ground subsidence and uplift, as well as downslope movements. Across the areas of observed geohazards, urban land cover types from the Copernicus (formerly GMES) EEA European Urban Atlas, e.g., continuous and discontinuous urban fabric and industrial units, show the highest average velocities away from the satellite sensor, and the smallest standard deviations (~ 0.7 – 1.0 mm/year). More rural land cover types such as agricultural, semi-natural and green areas reveal the highest

spatial variability (up to ~ 4.4 mm/year), thus suggesting greater heterogeneity of observed motion rates within these land cover types. Areas of observed motion in the PSI data for which a geological interpretation cannot be found with sufficient degree of certainty are also identified, and their possible causes discussed. Although present in Greater London, some geohazard types such as shrink–swell clays and ground dissolution are not highlighted by the interpretation of PSI annual motion rates. Reasons for absence of evidence of the latter in the PSI data are discussed, together with difficulties related to the identification of good radar scatterers in landsliding areas.

Key words: Geohazard, persistent scatterer interferometry, ground motion, InSAR, monitoring, land surface processes.

1. Introduction

Geohazards and their impacts in the United Kingdom (UK) have long been discussed in the literature. GIBSON *et al.* (2013) analyse aspects related to management of landslide hazards in an environment considered as low-risk, but where the financial loss from such a hazard is likely to be in excess of £10 million per year. FARRANT and COOPER (2008) investigate geological properties of soluble rocks, and report on karstic features observed in Carboniferous limestone, chalk and Permo-Triassic gypsum and halite. Flooding and storms occurring in vulnerable floodplains and coastal areas have large economic impacts, and single hydro-meteorological events have caused damage of over £3 billion (PITT 2008). Predominantly affecting the southeast of the country, volume changes of clay soils and mudrocks in response to variations in moisture content are considered the cause of the largest financial impact in the UK, with costs up to £500 million in a single year

¹ British Geological Survey, Natural Environment Research Council, Nicker Hill, Keyworth, Nottinghamshire NG12 5GG, UK. E-mail: fcigna@bgs.ac.uk; hann@bgs.ac.uk; lbateson@bgs.ac.uk

² CGG, NPA Satellite Mapping Ltd., Crockham Park, Edenbridge, Kent TN8 6SR, UK. E-mail: harry.mccormack@cgg.com; claire.roberts@cgg.com

(JONES and TERRINGTON 2011). The correlation between geotechnical and mineralogical factors and the shrink–swell susceptibility of the UK has been analysed and discussed widely (e.g., JONES and JEFFERSON 2012), and major relationships between the number of subsidence claims due to shrinkage and historical records of both precipitation and average temperatures have been found (HARRISON *et al.* 2012).

The British Geological Survey (BGS) has undertaken natural geohazard susceptibility mapping for Great Britain, and produced the GeoSure data set (BOOTH *et al.* 2010; WALSBY 2008). Developed at a scale of 1:50,000, this data set provides information about potential natural ground movement resulting from collapsible deposits, compressible ground, landslides (GIBSON *et al.* 2013), running sand, shrink–swell (HARRISON *et al.* 2012) and soluble rocks (COOPER *et al.* 2011). Susceptibility is classified using an *A* (lowest) to *E* (highest) rating for each of these six geohazard types (BGS 2014).

Depending on their causes, geohazards can be observed within areas of high natural geohazard susceptibility or even areas where susceptibility is low. For instance, land subsidence induced by anthropogenic activities such as mining or tunnelling can occur in areas with low susceptibility to ground compaction, where motions at the surface can occur in response to artificial changes in the in situ stress induced by the excavation and removal of subsurface material. Similarly, changes in the pore water pressure due to groundwater abstraction for domestic use, or water levels control during engineering and mining works, can alter local conditions in the effective stress and result in ground surface motions. Surface evidence of these processes in the UK was recently investigated by processing satellite synthetic aperture radar (SAR) imagery and interpreting their derived ground motion data together with a range of geological layers and information (e.g., BANTON *et al.* 2013; BATESON *et al.* 2014; CULSHAW *et al.* 2006; LEIGHTON *et al.* 2013; SOWTER *et al.* 2013). A feasibility study with nationwide coverage has also been carried out by CIGNA *et al.* (2014) to assess the potential of ERS-1/2 and ENVISAT C-band SAR-based imaging of the land-mass of Great Britain, by analysing archive data availability, simulating geometric distortions and modelling land cover control on the success of SAR,

interferometric SAR (InSAR) and persistent scatterer interferometry (PSI) applications.

For the area of London and Thames estuary, the DEFRA/EA R&D Land Levels project analysed land level changes using ERS-1/2 and ENVISAT PSI ground motion data from March 1997 to December 2005. A variety of regional to local-scale controlling factors on the rates of these changes were found, ranging from near-surface to deep-seated mechanisms, and with a variety of temporal scales, from <10 to over 100,000 years duration (ALDISS *et al.* 2014; BINGLEY *et al.* 2007). Geological interpretation of spatial correlations between the larger variations in satellite data and various geological data sets allowed the identification of ‘domains’ of approximately uniform vertical ground velocity and the identification of major lineaments within the data distribution. This project examined the data at up to 1:20,000 scale, whereas higher spatial scales and smaller variations in the PSI motion data were not interpreted (ALDISS *et al.* 2014).

Areas of observed and potential ground instability at the reference scale of 1:10,000 have been depicted for 52 of the largest towns across 27 countries within the European Union by the validated geohazard layers generated by the Geological Surveys of Europe in the framework of the PanGeo project (<http://www.pangeoproject.eu>). PanGeo was funded in 2011–2014 by the European Commission under the Space Theme, Seventh Framework Programme (FP7-SPACE), and led by Fugro—Nigel Press Associates (NPA), now CGG—NPA Satellite Mapping Ltd. Among these 52 towns, London (CIGNA *et al.* 2013c) and Stoke-On-Trent (JORDAN *et al.* 2013) were selected as targets for the UK, and the BGS was responsible for the generation of the respective geohazard layers. The objective of PanGeo was to enable free and open access to geohazard information in Europe in support of Copernicus, the European Earth Observation Programme. For each PanGeo town, the Geological Survey of the respective country has generated: (1) a polygon-wise ground stability layer (GSL) showing location, extent and typology of the observed and potential geohazards, and (2) the geohazard description (GHD) document, a supporting report that describes in detail the geological setting and places of interest affected by each geohazard, the

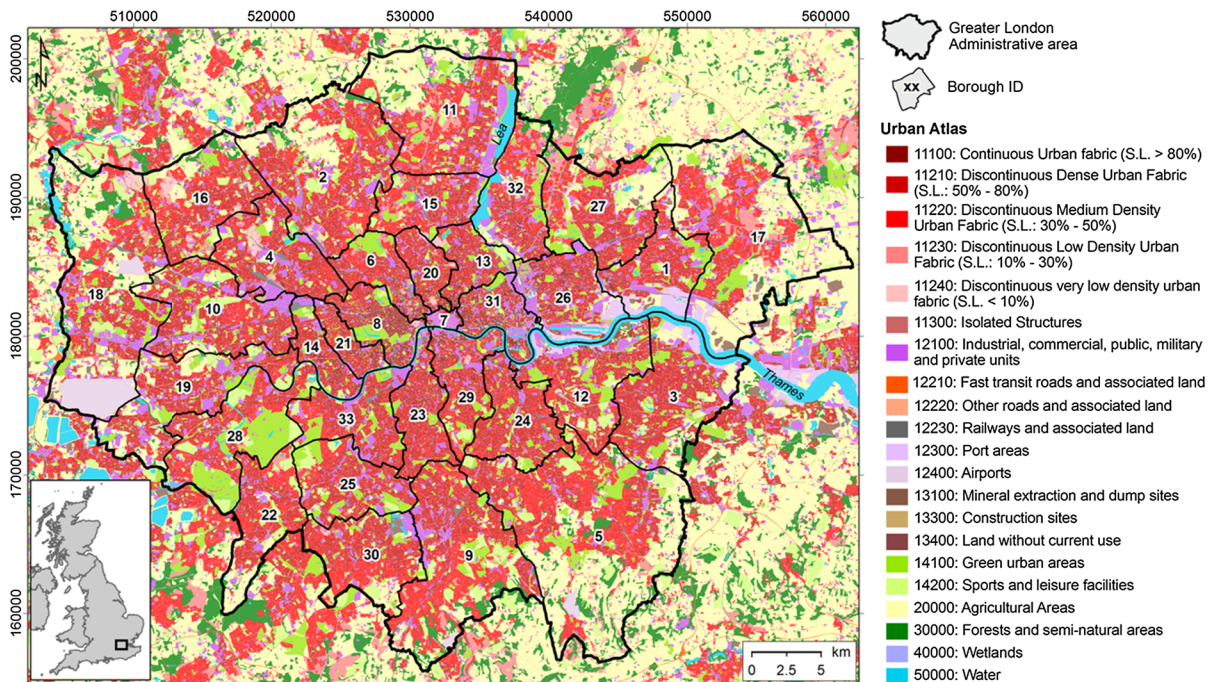


Figure 1

Land cover from the GMES EEA European Urban Atlas for Greater London administrative area and Boroughs; *S.L.* sealing layer. Borough IDs: 1 Barking and Dagenham, 2 Barnet, 3 Bexley, 4 Brent, 5 Bromley, 6 Camden, 7 City and County of the City of London, 8 City of Westminster, 9 Croydon, 10 Ealing 11 Enfield, 12 Greenwich, 13 Hackney, 14 Hammersmith and Fulham, 15 Haringey, 16 Harrow, 17 Havering, 18 Hillingdon, 19 Hounslow, 20 Islington, 21 Kensington and Chelsea, 22 Kingston upon Thames, 23 Lambeth, 24 Lewisham, 25 Merton, 26 Newham, 27 Redbridge, 28 Richmond upon Thames, 29 Southwark, 30 Sutton, 31 Tower Hamlets, 32 Waltham Forest, 33 Wandsworth. British National Grid; Projection: Transverse Mercator; Datum: OSGB 1936. GMES EEA Urban Atlas © EEA 2013, Directorate-General Enterprise and Industry (DG-ENTR), Directorate-General for Regional Policy

confidence and any additional evidence associated with the interpretation. All PanGeo GSL and GHD products have been made freely accessible and usable via a portal based on OneGeology Europe infrastructure that can be accessed at: <http://pangeo.brgm-rec.fr/pangeoportal>, or visualised in Google Earth via the PanGeo coverage map on: http://www.pangeoproject.eu/eng/coverage_map. Integration of the GSL with the Copernicus Land Theme's Urban Atlas (EC 2011) shows the land cover and use classes influenced by such hazards, and supports the end-users in the management of hazards and induced risks within the concerned areas.

Geological and other geospatial layers and information for the towns analysed within PanGeo were integrated with ground motion data generated from the processing of long temporal stacks of satellite SAR imagery, using PSI approaches (e.g., CROSETTO *et al.* 2010). When compared against other

monitoring data, the results of PSI techniques can achieve accuracies up to the level of a few mm/year, depending on surface characteristics of the processed area, quantity and quality of the input SAR imagery, and quality of the PSI processing. Findings of the European Space Agency (ESA) TerraFirma Validation study for the Alkmaar and Amsterdam sites in The Netherlands have shown that the observed overall accuracy of PSI average annual velocity was 1.0–1.8 mm/year (RMSE) for ERS-1/2 and ENVISAT data when compared against levelling (CROSETTO *et al.* 2008; HANSEN *et al.* 2008).

In this paper, we show the results of the generation of the PanGeo digital geohazard mapping product for Greater London. The total investigated site corresponds to the administrative area and extends ~1,580 km² (Fig. 1). This area includes the City of London and 32 other surrounding boroughs, within which a total population of more than 8

million inhabitants was censused in 2011, corresponding to an average of $\sim 5,200$ inhabitants/km².

We briefly describe the PanGeo methodology based on the Production Manual (BATESON *et al.* 2012) and illustrate the available input data for Greater London in Sect. 2. These include newly processed ERS-1/2 and ENVISAT PSI data sets showing the ground motion history of London over the last two decades. In Sect. 3, building upon the results of the PanGeo products generation, we analyse the potential of PSI, geological data and the PanGeo methodology to delineate areas of observed geohazards. Some types of geohazards that were not highlighted by the interpretation of annual motion rates from the PSI data, such as shrink–swell clays and dissolution, are considered in Sect. 3.4, where the reasons for absence of evidence of the latter in the PSI average motion velocities are also discussed, together with difficulties related to the identification of good radar scatterers in landsliding areas, where land cover exerts significant control on the success of conventional PSI techniques. Areas of potential instability due to natural geohazards have not been mapped for the UK PanGeo towns, as these are already delineated for all Great Britain at the 1:50,000 scale through the GeoSure data sets, for which further information is provided in Sect. 3.4.

2. Interpretation Methodology and Input Data

The interpretation and geohazard mapping approach employed for the delineation of observed geohazards in Greater London, conforms to the step-by-step methodology that is extensively described by BATESON *et al.* (2012) in the PanGeo Production Manual. The latter is a freely downloadable document that was distributed to the Geological Surveys to support the generation of their GSL by following instructions and procedures in accordance with the PanGeo Product Specification (BATESON 2013), in addition to specific training workshops and related material, which can be accessed at: <http://www.pangeoproject.eu/eng/educational>.

All the GSL polygons are attributed with classifications and hazard categories compliant with the Natural Risk Zones data specification of INSPIRE

(EC-JRC, 2013), which are also used in the project portal to provide a summary of the geohazard identified within the area. Geohazard categories considered by PanGeo are ‘Deep Ground Motions’, ‘Natural Ground Instability’, ‘Natural Ground Movement’, ‘Anthropogenic Ground Instability’, ‘Other’ (i.e., their geological explanation does not fit into any of the previous categories) and ‘Unknown’ (i.e., of which a geological interpretation cannot be found with sufficient degree of certainty), and each includes a number of hazard types. These conform to the Glossary of terms for PanGeo, available within the Product and Service Specification report of the project (BATESON 2013). A measure of the confidence in the interpretation is attributed to each geohazard, by using a scale of ‘low’, ‘medium’ and ‘high’ depending on the number of data sets used in the interpretation, or ‘external’ for those geohazards imported from an external source (e.g., landslide inventory). The determination method refers to the main information source that has been used to identify the geohazard, and is classified in PanGeo as: ‘Observed in PSI’, ‘Observed in Other Deformation Measurement’ (e.g., levelling, GPS), ‘Observed in Geology Field Campaigns’ or ‘Potential’. Full details and a step-by-step methodological approach are described in the PanGeo Production Manual by BATESON *et al.* (2012).

The identification of geohazards in Greater London was performed through combined interpretation of geological, geomorphologic, land use and other geospatial layers available at the BGS (cf. CIGNA *et al.* 2013c), together with satellite PSI ground motion data for the 18-year long period between 1992 and 2010 (see Sect. 2.1). Background input data used to map geohazards include Ordnance Survey (OS) topographic maps at 1:10,000–1:50,000 scales, 0.25-m resolution aerial photographs, 5-m resolution NEXTMap[®] DEM, the Digital Geological Map of Great Britain (DiGMapGB) at 1:625,000 to 1:10,000 scales (SMITH, 2013), the Superficial Deposits Thickness Model (SDTM) at 1:50,000 scale (LAWLEY and GARCIA-BAJO 2009), the National Landslide Database (NLD; FOSTER *et al.* 2012) and Karst Database (FARRANT and COOPER 2008), and groundwater pumping records from recent surveys carried out by the Environment Agency (EA 2007, 2010).

Table 1

Main characteristics of the PSI data sets employed for the generation of the GSL of Greater London

Data stack	No. scenes	Period (day/mo/yr)	Master scene	Georeference accuracy (m)	Reference point (lat, long)	PS coherence threshold	PSI processing area			GSL area	
							Area (km ²)	No. PS	PS density (PS/km ²)	No. PS	PS density (PS/km ²)
ERS-1/2 SAR ascending	27	19/06/1992–31/07/2000	13/01/1997	10	51.552°N, –0.113°E	0.53	2,500	730,254	292	615,950	386
ENVISAT ASAR descending	45	13/12/2002–17/09/2010	11/05/2007	10	51.554°N, –0.101°E	0.49	2,350	838,939	336	712,236	446

The results of the projects ESA GSE TerraFirma for the London H3 Modelled Product (BATESON *et al.* 2009; ESA 2009), and DEFRA/EA R&D Land Levels project results (ALDISS *et al.* 2014; BINGLEY *et al.* 2007) were also incorporated into the interpreted geohazard polygons of the GSL. The latter include average vertical ground motion information for ‘domains’ of uniform land level change that were identified based on an absolute gravimetry (AG) and GPS-aligned, ERS-ENVISAT-combined PSI product covering the period between 1997 and 2005, and processed by CGG—NPA Satellite Mapping, Ltd.

2.1. ERS-1/2 and ENVISAT Interferometric Point Target Analysis

To generate two new data sets of PSI ground motion data for Greater London, we employed the GAMMA SAR and Interferometry software, and in particular, the interferometric point target analysis (IPTA) algorithm, developed at GAMMA Remote Sensing and Consulting AG in Switzerland (WERNER *et al.* 2003). IPTA exploits the spatial and temporal characteristics of interferometric phase signatures of ground targets that exhibit point-like scattering behaviour and remain coherent over the monitored period, to estimate their ground motion velocities, time histories, terrain heights, and relative atmospheric path delays. This technique was recently used to monitor a variety of geological processes and man-made geohazards, including landsliding, ground subsidence, deep-level mining and structural instability (e.g., GIGLI *et al.* 2012; STROZZI and AMBROSI 2007; TEATINI *et al.* 2007; WEGMULLER *et al.* 2010). As input

for the IPTA processing, we used the following data stacks of C-band, VV polarized SAR imagery acquired from sun-synchronous near-polar orbits and with 35 days nominal repeat cycle (Table 1):

1. 27 ERS-1 and ERS-2 SAR scenes acquired between 19/06/1992 and 31/07/2000 in ascending mode, along the satellite track 201; and
2. 45 ENVISAT advanced SAR (ASAR) Image Mode IS2 scenes acquired between 13/12/2002 and 17/09/2010 in descending mode, along the satellite track 51.

The inclination of both ERS-1/2 and ENVISAT satellite ground tracks at the SAR scene centre was $\sim 14^\circ$ with respect to the S–N axis at the latitude of Greater London, and the incidence angle of the employed sensor modes was $\sim 23^\circ$ measured from the vertical direction. This means that the employed LOS were able to estimate purely vertical motions as $\sim 92\%$ of their actual amount, E–W motions as $\sim 38\%$, and N–S as only $\sim 9\%$.

The processing followed the iterative methodology described by WERNER *et al.* (2003), and was carried out based on a selected number of candidate points in the radar imagery that were persistent over the observation time period and dominated the backscattering within the resolution pixels. The 90 m resolution Shuttle Radar Topography Mission (SRTM) Digital Surface Model (DSM) by NASA-JPL was used to simulate the initial topographic phase components, and a simple linear model of phase variation through time was chosen to extract phase signals relating to ground displacements.

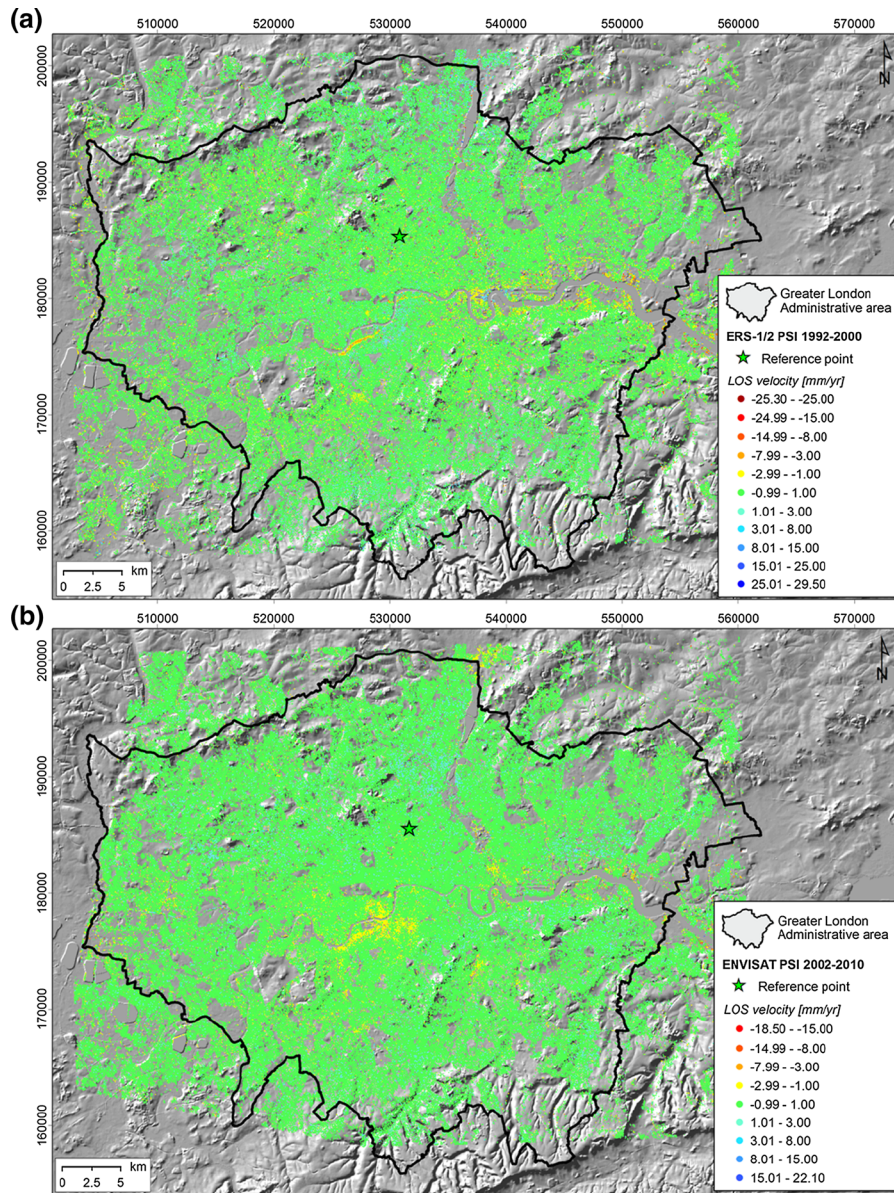


Figure 2

Average motion velocities in **a** 1992–2000 and **b** 2002–2010 for Greater London, estimated along the line-of-sight of, respectively, ERS-1/2 satellites in ascending mode and ENVISAT in descending mode. Refer to Table 1 for detailed processing statistics. *Green PS* are considered stable with respect to the reference point location, whereas *yellow to dark red PS* indicate motions recorded away from the sensor, and *light to dark blue* indicate motions towards the sensor. PSI data are overlapped onto shaded relief of NEXTMap[®] DTM at 50 m resolution. British National Grid; Projection: Transverse Mercator; Datum: OSGB 1936. NEXTMap[®] Britain © 2003, Intermap Technologies Inc., All rights reserved

Step-wise iterative processing using height corrections, linear motion rates, standard deviations and residual phases, allowed us to progressively improve the different phase components, and to extract a total of 730,254 ERS-1/2 persistent scatterers (PS),

corresponding to an average density of 292 PS/km² across the ~2,500 km² processing area, and 386 PS/km² within the administrative area of Greater London. The processing of the ENVISAT stack identified 838,939 targets, hence 336 PS/km²

over the respective processing area of $\sim 2,350 \text{ km}^2$, and 446 PS/km^2 in Greater London (Fig. 2). Despite the difference in the number of scenes populating the two stacks, the observed number and density of targets over the GSL area are similar, and amount to $\sim 400 \text{ PS/km}^2$ per data set. The somewhat greater density observed for the ENVISAT results is likely due to the larger number of scenes composing the ENVISAT stack, as opposed to the ERS stack. Indeed, higher numbers of input scenes generally result in PS data sets with both higher quality and reliability, and denser networks of good reflectors. In this particular case, the different coherence thresholds used to extract the final set of radar targets (i.e., 0.53 for ERS and 0.49 for ENVISAT) clearly had an impact on the final number of points, with the ENVISAT data set more likely to have more scatterers due to the lower threshold employed. Bearing in mind that the selection of the optimal coherence thresholds is a trade-off between the quality and the number of point targets composing the resulting data set, for the area of Greater London, a higher coherence threshold during the ERS-1/2 processing was chosen. This was done in order to minimise the inclusion of lower quality targets in the final results, accounting for the smaller number of ERS-1/2 ascending mode SAR scenes available to perform the IPTA processing with respect to the more populated ENVISAT ASAR stack.

Reference points for the PS data sets were identified at similar locations, i.e., WGS84 51.552°N , -0.113°E for ERS-1/2 and 51.554°N , -0.101°E for ENVISAT (see green stars in Fig. 2a, b). The locations were selected accounting for both the interferometric phase stability of the PS candidates and the geological setting of this sector of the area, which was considered a good site to reference all ground motion data to.

For over 95 % of the PS targets found within the GSL area, the standard deviations of the estimated annual velocity along the satellite LOS are between 0.09 and 1.09 mm/year in the ERS-1/2 data set, and between 0.17 and 1.13 mm/year in the ENVISAT data set (by assuming the data are normally distributed). Taking these values into account, we considered the PS points showing annual deformation

velocities along the LOS in the range of $\pm 1.0 \text{ mm/year}$ as ‘stable’ (i.e., green PS in Fig. 2a, b).

From the observation of average annual velocities across the administrative area, it is apparent that although the two PSI data sets revealed a general stability at the regional scale over both periods of 1992–2000 and 2002–2010, some areas show significant motions away from the satellite. In most cases, these are located along the Thames valley, and in the Fulham, Battersea and Clapham areas (Fig. 2). Minimum and maximum annual velocities observed within Greater London along the satellite LOS are -25.3 and $+29.5 \text{ mm/year}$ in the ERS-1/2 data set (1992–2000), and -18.5 and $+22.1 \text{ mm/year}$ in the ENVISAT data set (2002–2010). The distribution of average velocities also confirms the absence of regional trends or wide scale shifts that could have resulted from inappropriate selection of the reference location.

It is worth noting that the accuracy of ERS-1/2 and ENVISAT data sets can be assessed by comparing the resulting PSI ground motion velocities and time series against continuous GPS stations that operated in the study region during the same time intervals. For instance, vertical motion histories from GPS stations of the NERC-funded British Isles continuous GNSS Facility (BIGF; <http://www.bigf.ac.uk>) could be considered. This specific analysis would allow estimation of the reference accuracy of our results in Greater London, and correction of potential shifts due to the reference point selection and tilts that were artificially removed during the processing, though it is beyond the scope of this paper to analyse this aspect further.

3. Results and Discussion

Using the methodology described in Sect. 2, we identified a total of 25 geohazard polygons over Greater London, covering a total of $\sim 700 \text{ km}^2$, or $\sim 650 \text{ km}^2$ if excluding overlapping geohazards (Fig. 3; Table 2). In most cases, observed geohazards are identified as a single-part polygon, whereas in the case of landslides, the areas of motion are grouped into multi-part polygons sharing the same set of standardised PanGeo attributes.

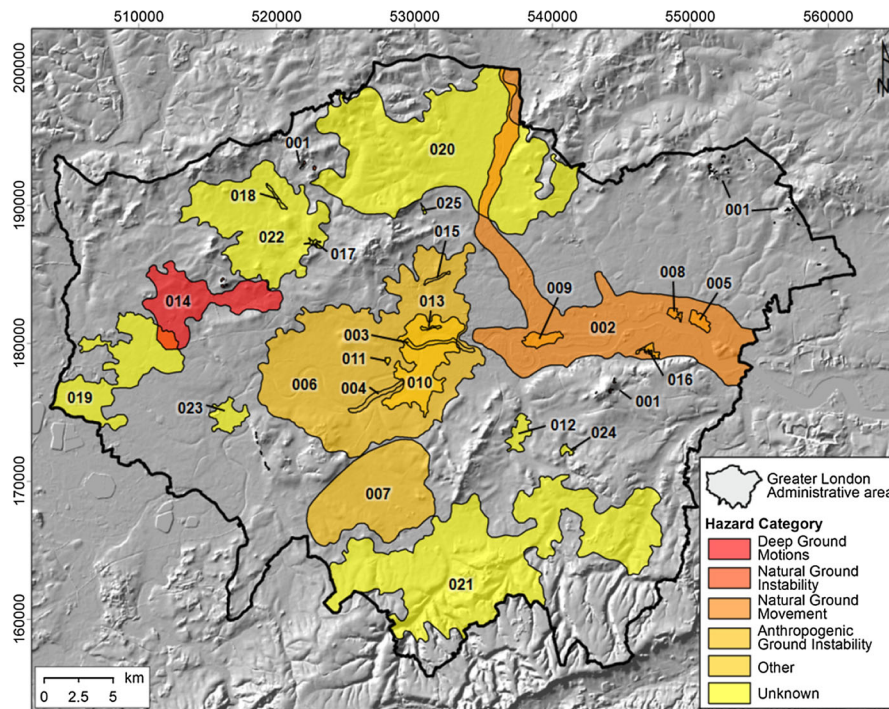


Figure 3

PanGeo Ground Stability Layer of Greater London: observed geohazards classified by Hazard Category and overlapped onto shaded relief of NEXTMap® DTM at 50 m resolution. Labels indicate the last three digits of the INSPIRE polygon IDs. Refer to Table 2 for detailed information and PSI ground motion statistics for each observed geohazard. British National Grid; Projection: Transverse Mercator; Datum: OSGB 1936. NEXTMap® Britain © 2003, Intermap Technologies Inc., All rights reserved

A range of geohazard types are observed, including both natural processes such as compaction of deposits on the River Thames flood plain and anthropogenic instability due to water abstraction and recent engineering works. There are nine areas of observed anthropogenic geohazards in total, including both the ‘Anthropogenic Ground Instability’ and the ‘Other’ hazard categories (see Sect. 3.2). Natural geohazards include three polygons (see Sect. 3.1) of ‘Natural Ground Instability’, ‘Natural Ground Movement’ and ‘Deep Ground Motion’, whereas 13 have unknown causes (see Sect. 3.3). In terms of ground area covered, the dominant geohazard is anthropogenic land subsidence caused by groundwater abstraction for a total of $\sim 300 \text{ km}^2$ (see Sect. 3.2.2), followed by natural compression of River Thames sediments over $\sim 105 \text{ km}^2$ (see Sect. 3.1.1). In many instances, geohazards of different categories and types overlap, thus indicating interaction of different processes (cf. Fig. 3).

As regards confidence in the interpretation, six high, six medium, 12 low and one external confidence level polygons are identified. As for the determination method, only one mapped polygon corresponds to geohazards observed by geology field campaigns (i.e., landslides from the NLD and DiGMapGB mass movement layer), whereas the remaining 24 correspond to areas observed in PSI data, 18 of which show subsidence and six of which show uplift. Ground motion statistics from ERS-1/2 and ENVISAT PSI data for all observed geohazards are summarized in Table 2. For each geohazard polygon, the maximum, minimum and average observed velocity of all PS points identified within its boundary are computed for both monitoring periods, with an understanding that different levels of homogeneity (or heterogeneity) can be observed within the various polygons; these are indicated by the observed standard deviation. The latter quantifies the dispersion of the annual velocity values for all the PS included

Table 2
Observed geohazards in Greater London: INSPIRE ID, hazard category and type, motion type, determination method, confidence level, total area, and ground motion statistics for each observed geohazard

INSPIRE ID (polygon ID)	Hazard	Category	Type	Motion type	Determination method	Confidence level	Area (km ²)	Observation date	ERS-1/2 data from 1992 to 2000				ENVISAT data from 2002 to 2010					
									No. PS	LOS velocity (VEL) (mm/year)	Avg	Min	Max	SD	No. PS	LOS velocity (VEL) (mm/year)	Avg	Min
PGGH_London_001	Natural Ground Instability		Landslide	Down slope	Observed Field Campaigns	External	0.52	14/10/2010 ^a	3	-3.32	-11.64	+1.05	7.20	5	-1.36	-1.87	-0.14	0.69
PGGH_London_002	Natural Ground Movement		Compressible Ground	Subsidence	Observed PSI	High	104.27	19/06/1992	33,597	-0.47	-19.19	+29.51	1.78	39,972	-0.51	-12.85	+9.09	1.00
PGGH_London_003	Anthropogenic Ground Instability		Underground Construction	Subsidence	Observed PSI	High	1.32	19/06/1992	883	-0.92	-15.89	+18.92	1.86	1,428	-1.16	-4.13	+2.16	0.74
PGGH_London_004	Anthropogenic Ground Instability		Underground Construction	Subsidence	Observed PSI	High	1.39	19/06/1992	870	-1.93	-14.04	+20.10	1.78	1,305	-1.81	-6.04	+0.62	0.64
PGGH_London_005	Anthropogenic Ground Instability		Made Ground	Subsidence	Observed PSI	High	1.38	19/06/1992	317	-3.23	-15.99	+5.57	3.45	400	-2.78	-10.64	+2.57	2.52
PGGH_London_006	Anthropogenic Ground Instability		Groundwater Abstraction	Subsidence	Observed PSI	High	146.65	13/12/2002	101,138	+0.19	-19.45	+22.47	1.15	130,813	-0.81	-9.22	+5.48	0.64
PGGH_London_007	Anthropogenic Ground Instability		Groundwater Abstraction	Subsidence	Observed PSI	High	47.17	19/06/1992	19,769	-0.14	-25.28	+20.11	1.16	23,477	-0.47	-8.43	+4.98	0.62
PGGH_London_008	Anthropogenic Ground Instability		Made Ground	Subsidence	Observed PSI	Medium	0.57	19/06/1992	261	-1.69	-11.92	+17.98	2.38	371	-1.72	-7.27	+1.39	1.32
PGGH_London_009	Other		Other	Uplift	Observed PSI	Medium	2.19	19/06/1992	377	+1.44	-2.36	+20.46	2.40	1,033	-0.96	-6.24	+1.79	1.04
PGGH_London_010	Other		Other	Uplift	Observed PSI	Medium	21.29	19/06/1992	17,747	+0.45	-16.28	+20.90	1.12	23,651	-0.96	-7.73	+4.72	0.68
PGGH_London_011	Unknown		Unknown	Subsidence	Observed PSI	Medium	0.14	19/06/1992	225	-1.34	-14.92	+0.37	1.15	218	-1.74	-4.83	+1.11	0.63
PGGH_London_012	Unknown		Unknown	Subsidence	Observed PSI	Medium	2.80	13/12/2002	1,774	-0.34	-11.52	+19.87	1.20	2,109	-1.21	-5.56	+1.72	0.70
PGGH_London_013	Unknown		Unknown	Subsidence	Observed PSI	Medium	0.23	13/12/2002	302	+0.43	-2.33	+7.09	0.63	476	-1.64	-5.38	+2.26	0.94
PGGH_London_014	Deep Ground Motions		Tectonic Movements	Uplift	Observed PSI	Low	26.63	19/06/1992	10,028	+0.40	-19.48	+22.23	1.22	15,049	-0.18	-7.74	+5.81	0.69
PGGH_London_015	Anthropogenic Ground Instability		Underground Construction	Subsidence	Observed PSI	Low	0.38	13/12/2002	272	+0.07	-4.55	+5.28	0.81	286	-1.09	-5.69	+4.76	0.85
PGGH_London_016	Unknown		Unknown	Subsidence	Observed PSI	Low	0.65	19/06/1992	428	-1.57	-12.76	+0.54	1.36	307	-1.59	-12.51	+1.33	1.51
PGGH_London_017	Unknown		Unknown	Subsidence	Observed PSI	Low	0.19	19/06/1992	164	-0.85	-9.40	+9.12	1.67	165	-1.33	-9.72	+1.36	1.17
PGGH_London_018	Unknown		Unknown	Subsidence	Observed PSI	Low	0.44	13/12/2002	325	-0.40	-20.12	+7.31	1.48	377	-1.10	-3.59	+2.31	0.66
PGGH_London_019	Unknown		Unknown	Subsidence	Observed PSI	Low	32.21	13/12/2002	7,045	+0.15	-17.52	+17.12	1.27	15,585	-0.74	-9.83	+4.90	0.69

Table 2 continued

INSPIRE ID (polygon ID)	Hazard	Motion type	Determination method	Confidence level	Area (km ²)	Observation date	ERS-1/2 data from 1992 to 2000						ENVISAT data from 2002 to 2010					
							Category	Type	Start	End	LOS velocity (VEL) (mm/year)			No. PS	LOS velocity (VEL) (mm/year)			No. PS
											Avg	Min	Max		SD	Avg	Min	
PGGH_London_020	Unknown	Uplift	Observed PSI	Low	127.16	19/06/ 1992	31/07/2000	59,918	+0.48	-19.47	+26.47	1.25	68,741	-0.09	-11.01	+8.43	0.62	
PGGH_London_021	Unknown	Uplift	Observed PSI	Low	126.85	19/06/ 1992	17/09/2010	52,695	+0.51	-22.62	+22.48	1.09	53,582	-0.10	-9.98	+5.65	0.55	
PGGH_London_022	Unknown	Subsidence	Observed PSI	Low	54.45	19/06/ 1992	17/09/2010	24,058	-0.28	-22.44	+18.81	1.15	28,561	-0.22	-9.72	+6.82	0.64	
PGGH_London_023	Unknown	Uplift	Observed PSI	Low	4.10	19/06/ 1992	31/07/2000	1,993	+0.60	-18.95	+17.63	1.11	2,375	-0.26	-5.06	+3.73	0.54	
PGGH_London_024	Unknown	Subsidence	Observed PSI	Low	0.52	13/12/ 2002	17/09/2010	202	+0.00	-4.01	+3.05	0.63	263	-1.15	-5.29	+1.03	0.64	
PGGH_London_025	Unknown	Subsidence	Observed PSI	Low	0.13	19/06/ 1992	17/09/2010	74	-0.59	-4.24	+8.63	1.60	31	-1.21	-3.97	+1.19	1.08	

^a Publication date of the DiGMapGB-50 V6.2 mass movements layer

within the boundaries of each geohazard polygon with respect to their spatial average. Low standard deviations indicate homogeneity, and high standard deviations indicate heterogeneity.

The Copernicus EEA European Urban Atlas (UA) shows that land use within the region is typified by continuous or discontinuous dense to medium density urban fabric, with sparse industrial and commercial units, and extended port areas present along the River Thames (EC 2011). Table 3 summarizes the total areas of each of the 20 UA land cover types present in Greater London, the fraction of these that are covered by PanGeo observed geohazard polygons, and respective ground motion velocity statistics during 1992–2000 and 2002–2010 based on the ERS-1/2 and ENVISAT PS data sets. Areas of observed geohazards mainly involve discontinuous urban fabric, with ~ 200 km² dense (UA code 11210) and ~ 94 km² medium density (UA code 11220) fabric. Industrial and commercial units are also widely affected by geohazards, with a total extent of ~ 88 km² UA code 12100 land cover polygons intersected by observed geohazards. Areas of continuous and discontinuous urban fabric, industrial, port areas and roads show the highest average velocities away from the satellite sensor and the smallest standard deviations (i.e., ~ 1.0 mm/year in the ERS-1/2, and ~ 0.7 mm/year in the ENVISAT data) across the UA polygons covered by observed geohazards. On the other hand, more rural land cover types, such as agricultural, semi-natural and green areas, mineral extraction and dump sites and forests, generally reveal the highest standard deviations across the UA polygons (up to ~ 4.4 mm/year in the ERS-1/2, and ~ 1.0 – 1.6 mm/year in the ENVISAT data), thus suggesting greater spatial variability of observed motions within these land cover types. Both subsidence and uplift are observed for the various UA types, although these are related to different geohazard categories and types, as discussed in the following sections.

It is worth noting that the London GSL provides information on geohazards identified from PSI data and geology field campaigns. The geohazard polygons within the GSL, therefore, represent geohazards observed by interpreting these input layers, and accounting for their specific temporal reference and

Table 3
Areal and velocity statistics for UA land cover types covered by PanGeo observed motions in Greater London

UA code	UA land cover type	Area (km ²)		ERS-1/2 data from 1992 to 2000					ENVISAT data from 2002 to 2010					
		Greater London (A)	Observed geohazards (B)	(B)/(A) (%)	No. PS	LOS velocity (VEL) (mm/year)		No. PS	LOS velocity (VEL) (mm/year)		No. PS	LOS velocity (VEL) (mm/year)		
						Avg	Min		Max	SD		Avg	Min	Max
11100	Continuous urban fabric (S.L. >80 %)	36.6	25.7	70	28,888	0.11	-21.89	+18.92	1.04	36,229	-0.70	-7.30	+5.80	0.67
11210	Discontinuous dense urban fabric (S.L. 50-80 %)	432.2	199.2	46	131,540	0.19	-25.28	+21.57	1.10	155,559	-0.47	-12.28	+7.09	0.67
11220	Discontinuous medium density urban fabric (S.L. 30-50 %)	207.9	93.9	45	45,539	0.44	-21.09	+26.47	1.11	50,465	-0.18	-11.01	+5.72	0.59
11230	Discontinuous low density urban fabric (S.L. 10-30 %)	28.6	10.5	37	4,643	0.45	-18.08	+20.73	1.23	5,399	-0.16	-9.42	+5.04	0.60
11240	Discontinuous very low density urban fabric (S.L. <10 %)	7.0	2.4	34	1,191	-0.05	-14.93	+21.25	1.45	1,621	-0.36	-5.32	+2.14	0.72
11300	Isolated structures	1.2	0.1	6	28	0.38	-0.45	+1.22	0.42	30	-0.11	-1.40	+1.37	0.62
12100	Industrial, commercial, public, military and private units	170.3	87.9	52	63,971	0.13	-22.44	+22.48	1.31	76,504	-0.45	-12.51	+9.09	0.84
12210	Fast transit roads and associated land	2.4	0.5	21	127	-0.18	-15.17	+10.48	2.35	169	-0.65	-7.83	+3.06	1.27
12220	Other roads and associated land	120.9	59.1	49	14,855	0.08	-19.37	+22.12	1.62	26,530	-0.51	-12.85	+6.82	0.79
12230	Railways and associated land	18.4	9.6	52	3,563	-0.05	-17.98	+20.34	1.94	5,355	-0.56	-9.98	+6.50	0.92
12300	Port areas	12.1	11.9	99	6,018	-0.70	-18.99	+20.93	1.87	7,164	-0.49	-8.20	+4.54	1.08
12400	Airports	16.3	8.2	50	1,543	0.01	-12.43	+17.12	1.41	2,555	-0.80	-9.53	+4.15	0.82
13100	Mineral extraction and dump sites	5.4	3.1	57	50	-0.07	-13.59	+18.54	3.97	74	-0.44	-7.29	+4.52	1.48
13300	Construction sites	3.1	2.3	74	1,386	0.27	-18.02	+19.43	1.24	136	-0.69	-4.19	+3.79	1.36
13400	Land without current use	2.2	1.3	59	184	-0.25	-13.75	+7.70	2.86	134	-0.93	-6.79	+0.84	1.35
14100	Green urban areas	146.0	46.3	32	2,313	-0.21	-18.72	+22.20	2.62	2,771	-0.64	-7.07	+4.90	0.95
14200	Sports and leisure facilities	116.6	39.9	34	2,665	-0.05	-19.47	+21.61	2.42	3,933	-0.47	-8.43	+4.88	0.92
20000	Agricultural areas, semi-natural areas and wetlands	189.8	25.8	14	527	-0.60	-17.97	+21.38	3.66	708	-0.77	-10.57	+4.09	1.64
30000	Forests	40.3	6.4	16	84	0.39	-17.09	+17.83	4.42	64	-0.37	-3.97	+1.10	0.85
50000	Water bodies	37.4	29.3	78	687	0.03	-19.19	+29.51	4.38	992	-0.43	-4.15	+3.37	0.72

The total area of each UA type in Greater London and the respective fraction affected by PanGeo observed geohazards is shown. Observed average, minimum, maximum and standard deviation for the ERS-1/2 and ENVISAT LOS ground motion velocities during 1992-2000 and 2002-2010 are also summarized for each UA land cover type

spatial scales and resolutions. This aspect is discussed in detail in Sect. 3.4. The PanGeo product also needs to be used in conjunction with geohazard susceptibility maps indicating areas of potential geohazards. As mentioned above, for Great Britain, these are provided by the BGS through the GeoSure data set (BOOTH *et al.* 2010; WALSBY 2008) for the six natural ground movement types of collapsible deposits, compressible ground, landslides, running sand, shrink–swell and soluble rocks.

3.1. Observed Natural Geohazards

Topography, geomorphology and geology of Greater London are controlled by the presence of the drainage network formed by the River Thames and its tributaries. This network is associated with an alluvial tract that lies at about 10 mOD in the west of the area, falling towards sea level to the east of the district. Gently sloping valley sides rising to approximately 30 mOD border the riparian zones. The north-eastern sector is characterised by a dissected plateau at about 100 mOD, whilst to the south of the River Thames, the land rises gently southwards. Alluvium, till, marine, glaciofluvial and river terrace deposits of Quaternary age are mapped within the administrative area. Interfluves in the north-west of the area are formed of dissected London Clay capped, in places, by fine-grained sands of the Bagshot Formation. Sparse outliers of glaciofluvial deposits are also present. The ground rises to a dissected plateau of till at about 100 mOD in the north-east of the study area. South of the River Thames, the land rises gently across the London Clay towards the southern extremity of the district, where white to grey Chalk is present at surface. Clays and some sands and gravels of the Lambeth Group and silts and sands of the Thanet Sand Formation are present at the surface between the areas of London Clay and Chalk (ELLISON *et al.* 2004).

The presence of alluvium in the river flood plain, extensive areas of clays at the surface, lithologies containing loosely packed sandy layers, slopes prone to landsliding, and deep-seated tectonic structures make this area particularly susceptible to natural hazards. Observed natural geohazards, based on the two PSI ground motion data sets for 1992–2000 and

2002–2010, and geology field campaigns, encompass the three main categories of ‘Natural Ground Movement’, ‘Natural Ground Instability’ and ‘Deep Ground Motions’ (Table 2), and in Greater London include a total of three PanGeo geohazard polygons, classified as ‘Compressible Ground’, ‘Landslide’ and ‘Tectonic Movements’, respectively, according to the PanGeo Geohazard Glossary (BATESON 2013).

3.1.1 Compressible Ground

Centred upon the River Thames and its tributary, the River Lea in the east of Greater London, is a 101 km², low-lying area with typically gentle relief, identified in PanGeo as geohazard polygon ‘PGGH_London_002’ and indicating ground motion caused by compressible deposits (Fig. 4). The observed ground motion extends 20 km inland from its most easterly limit at the administrative boundary near Erith, and at its widest, reaches 6 km, diverging from the channel of the River Thames by a maximum of 3 km. Landmarks such as the London Docklands, Millennium dome, Olympic Park, Cutty Sark, London City Airport, Thames Barrier and the Blackwall Tunnel are present in this area, and regions of water, port areas, discontinuous dense urban fabric and discontinuous medium density urban fabric predominate, although land cover within this area is generally varied.

The area of instability coincides with extensive areas of relatively thick deposits of Holocene alluvium in the flood plain and salt marshes of the Rivers Lea and Thames. These overly deposits are of the London Clay Formation, Lambeth Group, Thanet Sand Formation and the Seaford Chalk Formation and Newhaven Chalk Formation. The Holocene deposits are susceptible to progressive subsidence from compaction, drying and resulting compression.

Analysis of average motion velocities from 1992 to 2010 for the areas of the Hornchurch, Rainham, Aveley and Wennington Marshes, where the thickness of the superficial deposits is up to ~40 m, reveals that the PSI-derived motion velocities increase up to –15 mm/year, with increasing deposit thickness and presence of made ground (Fig. 4). On the other hand, there seems to be no significant correlation between sediment thickness and the

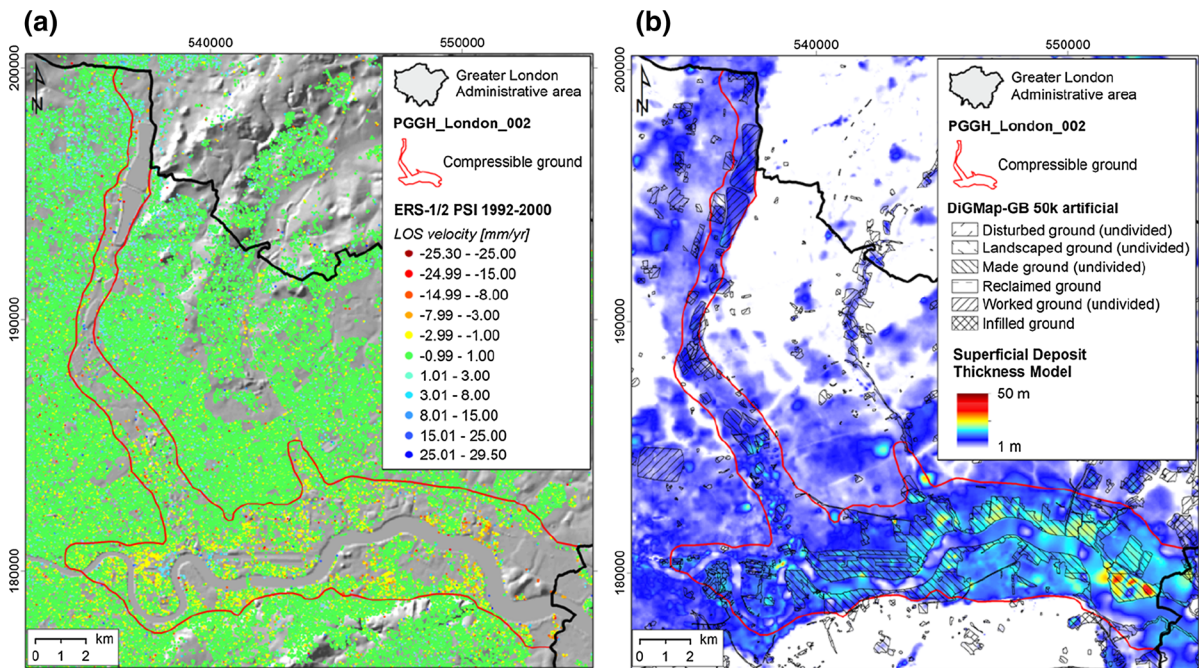


Figure 4

a Average motion velocities from 1992 to 2000 for polygon PGGH_London_002, estimated along the line-of-sight of ERS-1/2 satellites in ascending mode, overlapped onto the shaded relief of NEXTMap[®] DTM at 50 m resolution. **b** Artificial deposits from DiGMapGB at 1:50,000 scale, onto Superficial Deposit Thicknesses derived from the BGS Superficial Deposit Thickness Model (SDTM). Refer to Table 2 for detailed information and PSI ground motion statistics. British National Grid; Projection: Transverse Mercator; Datum: OSGB 1936.

NEXTMap[®] Britain © 2003, Intermap Technologies Inc., All rights reserved. Geological materials © NERC, All rights reserved

amount of subsidence based on PSI velocity values in the upper parts of river catchments including the River Thames upstream of Tower Bridge, where alluvium is <5 m thick. This confirms observations by BINGLEY *et al.* (2007).

The identified geohazard polygon corresponds well with domains '5F' and '6D' identified by ALDISS *et al.* (2014). Ground motion in the domains identified by ALDISS *et al.* (2014) reached vertical motion velocities in the order of -1.30 ± 0.95 mm/year along the River Lea and -1.99 ± 1.87 mm/year along the Thames in the period from 1997 to 2005. This means that the spatial average velocity of all PS targets within the boundaries of these domains was -1.30 (domain '5F') and -1.99 mm/year (domain '6D'), with observed deviations from these values equal to 0.95 and 1.87 mm/year, respectively. The latter indicate that for 68.2 % of the PS targets within the boundaries of these two domains, the observed annual velocities were, in turn, in the ranges of -2.25 to -0.35 mm/year, and -3.86 to -0.12 mm/year

during 1997–2005 (by assuming normal distribution of the PS velocities within the polygon boundary). The average LOS velocities observed by analysing our ERS-1/2 and ENVISAT IPTA targets within the mapped geohazard polygon boundary are -0.47 ± 1.77 mm/year during 1992–2000, and -0.51 ± 1.00 mm/year during 2002–2010 (Table 2). These values indicate that the majority of the targets reveal annual velocities in the range of -2.24 to $+1.30$ mm/year from 1992 to 2000, and -1.51 to $+0.49$ mm/year from 2002 to 2010. A maximum negative LOS PS velocity of -19.19 mm/year is achieved between 1992 and 2000, amounting to a maximum total displacement of 153.5 mm along the LOS over the 8-year period. By assuming a purely vertical motion direction for this area, the projection of the LOS values to the vertical direction can be performed by simply rescaling LOS observations by a factor of 1.09 (by dividing the LOS values by the cosine of the 23° incidence angle). This rescaling results in observed spatial averages within the polygon boundary of

-0.51 ± 1.93 mm/year from 1992 to 2000, and -0.56 ± 1.09 mm/year from 2002 to 2010.

3.1.2 Landslides

Areas of observed landslides in Greater London cover ~ 0.53 km² and are mainly located in the Havering, Barnet, Ealing, Greenwich, and Richmond upon Thames Boroughs. These have been categorized in the multi-part geohazard PanGeo polygon 'PGGH_London_001', and include 37 individual landslide deposits. The latter were mapped by BGS at 1:10,000 scale based on geology field campaigns and digital stereoscopic aerial photo interpretation, digital field data capture, terrestrial and airborne LiDAR, and differential GPS using a multi-stage methodology (EVANS *et al.* 2013), and recorded in the mass movement layer of the DiGMapGB (BECKEN and GREEN 2000; SMITH 2013), and the NLD (FOSTER *et al.* 2012). Mapped landslide deposits include both phenomena active at the time of survey, and older, inactive and relict landslides that are identified based upon the identification of certain morphological and sedimentological characteristics, and not necessarily on the observation of motion.

The majority of landslide features in Greater London occur on deposits of the London Clay Formation, often in close proximity to the boundary with overlying, more-permeable units. Landsliding mechanisms within the area vary from flows to multiple, successive rotational slides (FORSTER *et al.* 2003), and the ages of the features range between old (<1,000 years) and recent (<100 years). The Claygate Member of the London Clay is particularly prone to failure, and possesses a high plasticity and high water content on account of water-bearing sand layers and the uppermost deposits of the underlying London Clay (ELLISON *et al.* 2004; FORSTER 1997; SUMBLER 1996). In addition, where the Claygate Member is overlain by water-bearing sand in the Bagshot Formation, spring lines may develop, potentially raising pore-water pressure in material below. Many London Clay slopes steeper than 3° are covered by a veneer of head composed of redeposited London Clay including the Claygate Member, and may potentially be unstable (ELLISON *et al.* 2004).

Analysis of the ERS-1/2 and ENVISAT PSI data distribution for landslides in Greater London shows extremely low densities to absence of radar targets within the landslide deposit areas (Table 2). A total of only three ERS and five ENVISAT PS were identified for the 37 landslide deposits. To the south of the River Thames, within the Greenwich Borough, PSI data for one landslide deposit record velocities of -1.87 , -1.63 , -1.51 mm/year between 2002 and 2010 (Fig. 5a). Ground motion due to landsliding has been observed on the flanks of Shooters Hill, Eltham Common. The hill itself is capped by Pleistocene sand and gravel of the Stanmore Gravel Formation, Crag Group (Fig. 5b). The landslide deposits possess maximum elevations of ~ 100 m a.s.l., variable aspects (15°–105°) and widths ranging between 74 and 205 m. Four occur in the London Clay Formation and one in the Claygate Member. The observed LOS velocities for the three PS targets mentioned above correspond, respectively, to 4–5 mm/year if re-projected along the steepest slope direction of the respective locations, and suggest that part of the deposit still shows signs of activity.

In the Richmond-upon-Thames Borough, seven landslide deposits situated along the western edge of Richmond Park are mapped in the DiGMapGB mass movement data set (Fig. 5d). The area is low-lying with typically gentle relief. However, slopes in the immediate vicinity of the landslides reach approximately 20%. The largest landslide feature possesses a width of 338 m, whilst maximum elevations of each of the polygons range between 48 and 24 mOD. Landslide failures occurred within the London Clay Formation of the Thames Group. Upslope of the majority of the deposits lies the Black Park Gravel Member of the Thames Valley Formation, and the close proximity of this more permeable unit to the failed areas suggests that hydrological regime and pore water pressure may influence ground stability in the area. PSI data show ground motion velocity of -11.63 mm/year between 1992 and 2000 for one PS located within one landslide deposit (Fig. 5c). Another PS located only 11 m away from the feature records -6.17 mm/year within the same time period, and indicates presence of motion outside the deposit, thus suggesting possible enlargement of the geohazard polygon,

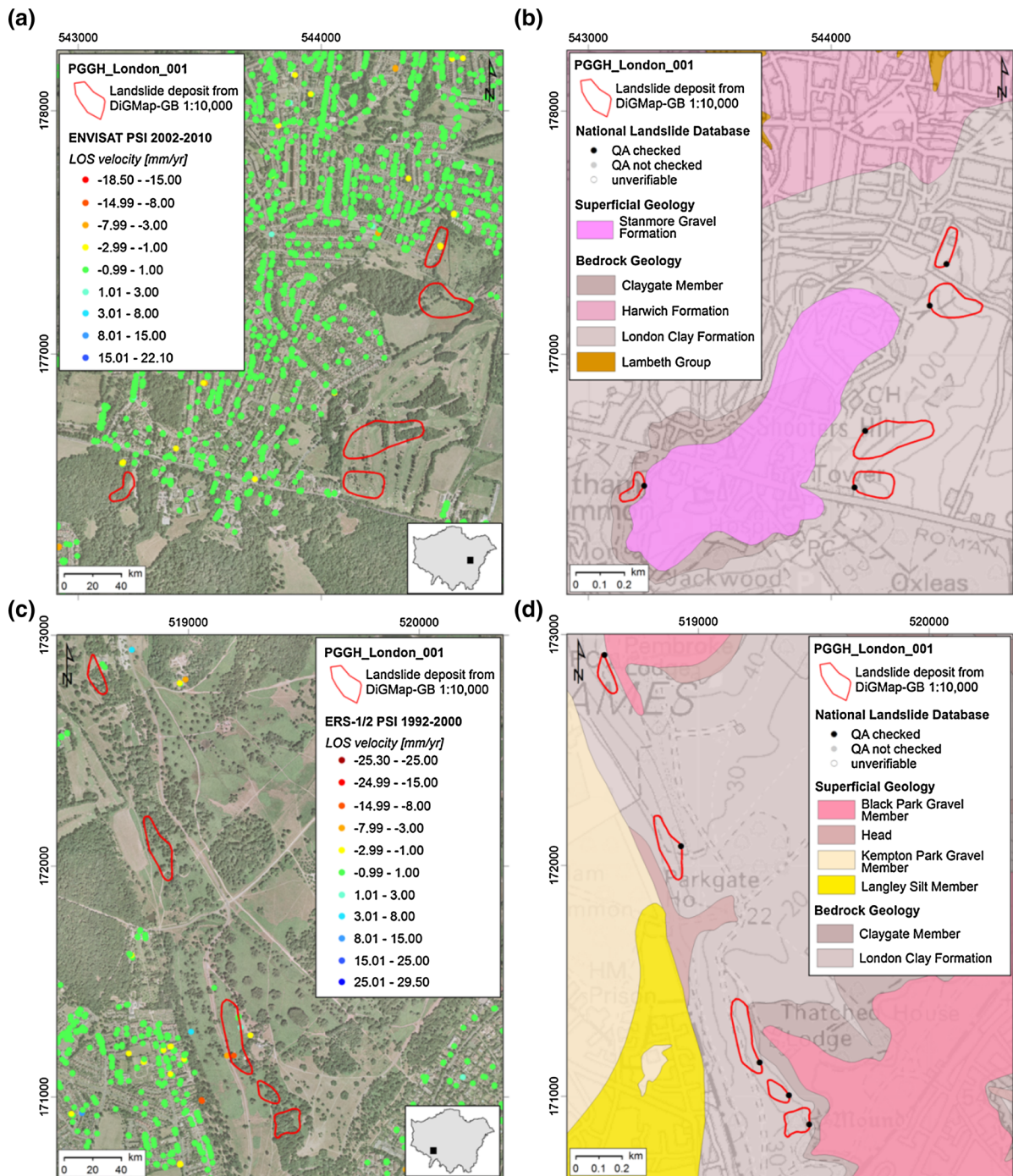


Figure 5

Examples of observed landslides in Greater London, delineated as PanGeo polygon PGGH_London_001: Average motion velocities in **a** 2002–2010 for landslide deposits in the Richmond upon Thames Borough and in **c** 1992–2000 for landslide deposits in the Greenwich Borough, estimated along the line-of-sight of ENVISAT in descending mode, and ERS-1/2 in ascending mode, respectively. Surface geology from the DiGMapGB at 1:50,000 scale for landslides in the **b** Richmond upon Thames and the **d** Greenwich Boroughs. PSI data are overlapped onto aerial photographs, whereas surface geology onto OS topographic map at 1:50,000 scale. *Insets* location within Greater London. Refer to Table 2 for detailed information and PSI ground motion statistics. British National Grid; Projection: Transverse Mercator; Datum: OSGB 1936. Geological materials © NERC, All rights reserved. OS data © Crown Copyright and database rights 2013. Aerial photography © UKP/Getmapping Licence No. UKP2006/01

which will be verified by analysis of geomorphological data and other field evidences.

Full details about all landslides deposits and PSI observations in other boroughs can be found in the GHD report for London, i.e., CIGNA *et al.* (2013c).

3.1.3 Tectonic Processes

Based upon the analysis of the ERS-1/2 and ENVISAT PS data, the regional gravity field of the area of London and ground motion domains of average vertical velocity from the DEFRA/EA joint project Land Levels (BINGLEY *et al.* 2007), we mapped a 26.63 km² area of observed deep ground motions related to tectonic movements. This area was identified as PanGeo geohazard ‘PGGH_London_014’ (Table 2), is centred upon the Greenholt area of west London, and was attributed a low confidence due to the level of uncertainty in the delineation of its overall extension.

Within the pre-Mesozoic basement, the Midlands Microcraton underlies the geohazard polygon. This terrane is characterised by the occurrence of Proterozoic rocks at relatively shallow depths, recorded recent isostatic uplift, and was delineated in terms of the generalised domain ‘G1’ by ALDISS *et al.* (2014). Gravity data that were processed using gravity stripping to the base of the Mesozoic succession,

enhanced variations in the regional Bouguer gravity anomaly field, which largely relates to Palaeozoic or Proterozoic age geological formations beneath the Chalk Group (ALDISS *et al.* 2014). For domain ‘G1’, a gravity ‘high’ (i.e., where the mass of underlying rock is greater than average) suggests presence of relatively dense rocks close to the surface, and that deep-seated tectonic structures could have causative relationship with the observed ground motions (Fig. 6b).

The ERS-1/2 PS results for 1992–2000 identify ground uplift with $+0.40 \pm 1.22$ mm/year LOS velocity for the PS targets within the polygon boundary (Fig. 6a), and an observed maximum of $+22.23$ mm/year, which corresponds to a total movement of 18 cm towards the satellite sensor over the monitored interval. Analysis of ground motions between 2002 and 2010 reveals a general change in the deformation trend of the geohazard polygon. Subsidence is recorded by the ENVISAT PS results, with -0.18 ± 0.69 mm/year for the PS within the polygon, and -7.74 mm/year observed peak velocities, due to either an inversion of the motion trend or, more likely, the presence of another geohazard type, overlapped onto (and thus masking) the existing uplift. Comparison with ground motion domains from ALDISS *et al.* (2014) suggests that the unstable area corresponds with domain ‘1’ identified from AG-

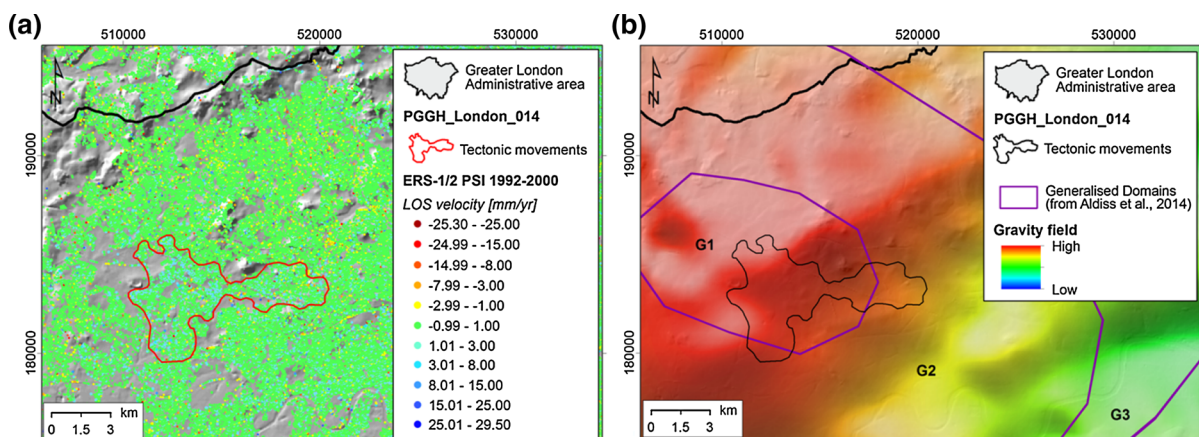


Figure 6

a Average motion velocities from 1992 to 2000 for PGGH_London_014, estimated along the line-of-sight of ERS-1/2 in ascending mode; and **b** generalised vertical ground velocity domains and gravity field stripped to base of Mesozoic succession [modified from ALDISS *et al.* (2014)], overlapped onto shaded relief of NEXTMap[®] DTM at 50 m resolution. Refer to Table 2 for detailed information and PSI ground motion statistics, and Fig. 3 for location of this polygon within Greater London. British National Grid; Projection: Transverse Mercator; Datum: OSGB 1936. Geological materials © NERC, All rights reserved. NEXTMap[®] Britain © 2003, Intermap Technologies Inc., All rights reserved

aligned and GPS-aligned estimates of vertical velocity. These authors show that ground motion in this area reached a maximum velocity of +8.26 mm/year from 1997 to 2005, whilst the average velocity for the domain was +0.25 mm/year.

3.2. Observed Anthropogenic Geohazards

The surface geology in Greater London has been modified throughout the centuries by several anthropogenic factors that widely influence the local and regional patterns of ground motions; for example, engineering works and groundwater management. Ground motions related to anthropogenic factors have long been studied through the analysis of PSI data, including land motions induced by engineering works (e.g., ASTRIUM-GEO 2014; BERARDINO *et al.* 2000; KRIVENKO *et al.* 2012) and groundwater management (e.g., AMELUNG *et al.* 1999; BELL *et al.* 2008; CIGNA *et al.* 2012a; GALLOWAY *et al.* 1998; HERRERA *et al.* 2009).

Observed anthropogenic geohazards in Greater London include a total of nine PanGeo geohazard polygons, classified as 'Underground Construction', 'Made Ground', 'Groundwater Abstraction' and 'Other' (Table 2), according to the PanGeo Geohazard Glossary (BATESON 2013).

3.2.1 Underground Construction

Areas of observed geohazard associated with anthropogenic ground instability due to underground construction in Greater London consist of three polygons in the City of Westminster, Lambeth and Southwark areas of London ('PGGH_London_003'), the Wandsworth ('PGGH_London_004') and Islington ('PGGH_London_015') Boroughs (Fig. 7).

'PGGH_London_003' covers a linear area of 1.32 km² (Table 2) and crosses the River Thames in the region of Westminster Bridge, where a number of landmarks are present, such as sections of the British Rail Network, Waterloo Train Station, Buckingham Palace, the London Eye, the Tower of London and the Tate Modern Art Gallery. This area is a low-lying river flood plain with elevations generally in the range of 5 to 10 mOD, and the bedrock geology is characterised by the London Clay

Formation. Superficial deposits in the area include alluvium, peat, Kempton Park Gravel Formation, Langley Silt Member and Taplow Gravel Formation.

The unstable area indicated by the PSI data from both 1992 to 2000, and to a lesser degree, 2002 to 2010, corresponds with the location of the Jubilee Line Extension, which was constructed between 1993 and 1999 (BURLAND *et al.* 2001; PAGE 1995). In particular, the polygon area coincides with the 6 km-long line branch running between the Green Park and Bermondsey stations, opened at the end of 1999 (Fig. 7b). It is suggested that the motion observed from the PS data is due to ground compaction following underground engineering works of the Jubilee Line Extension project, and removal of subsurface material, which altered the support for the overlying terrain. STANDING and BURLAND (2006) report on tunnelling volume losses measured during construction of the tunnels for this line, and observe that losses higher than 3 % were measured in Westminster and in St James's Park, south of the lake, while north of St James's Park, losses were generally lower than 2 % as expected.

PSI data sets show motions away from the satellite sensor, indicating that land subsidence occurred during both time intervals, with LOS velocity for the PS targets within the polygon of -0.92 ± 1.86 mm/year during 1992–2000, and -1.16 ± 0.74 mm/year in the ENVISAT PS data from 2002 to 2010 (Fig. 7a). Maximum PS velocities estimated along the satellite LOS are approximately -15.9 mm/year from 1992 to 2000, amounting to a maximum total displacement of 13 cm over the 8-year period. Although average velocities decrease to < -4.1 mm/year during 2002–2010, motions due to the underground works are still identifiable from the ENVISAT monitoring data, and are discernible from the compaction of the alluvium affecting a wider sector of the city and due to groundwater abstraction (see Sect. 3.2.2). This geohazard polygon also corresponds well with domain '6C' identified by ALDISS *et al.* (2014).

A similar pattern in the PS ground motion data was observed for a 1.34 km², south-west trending, 4.5 km long area to the south of the River Thames in Wandsworth Borough ('PGGH_London_004'; Fig. 7c, d), in close proximity to the Battersea Park,

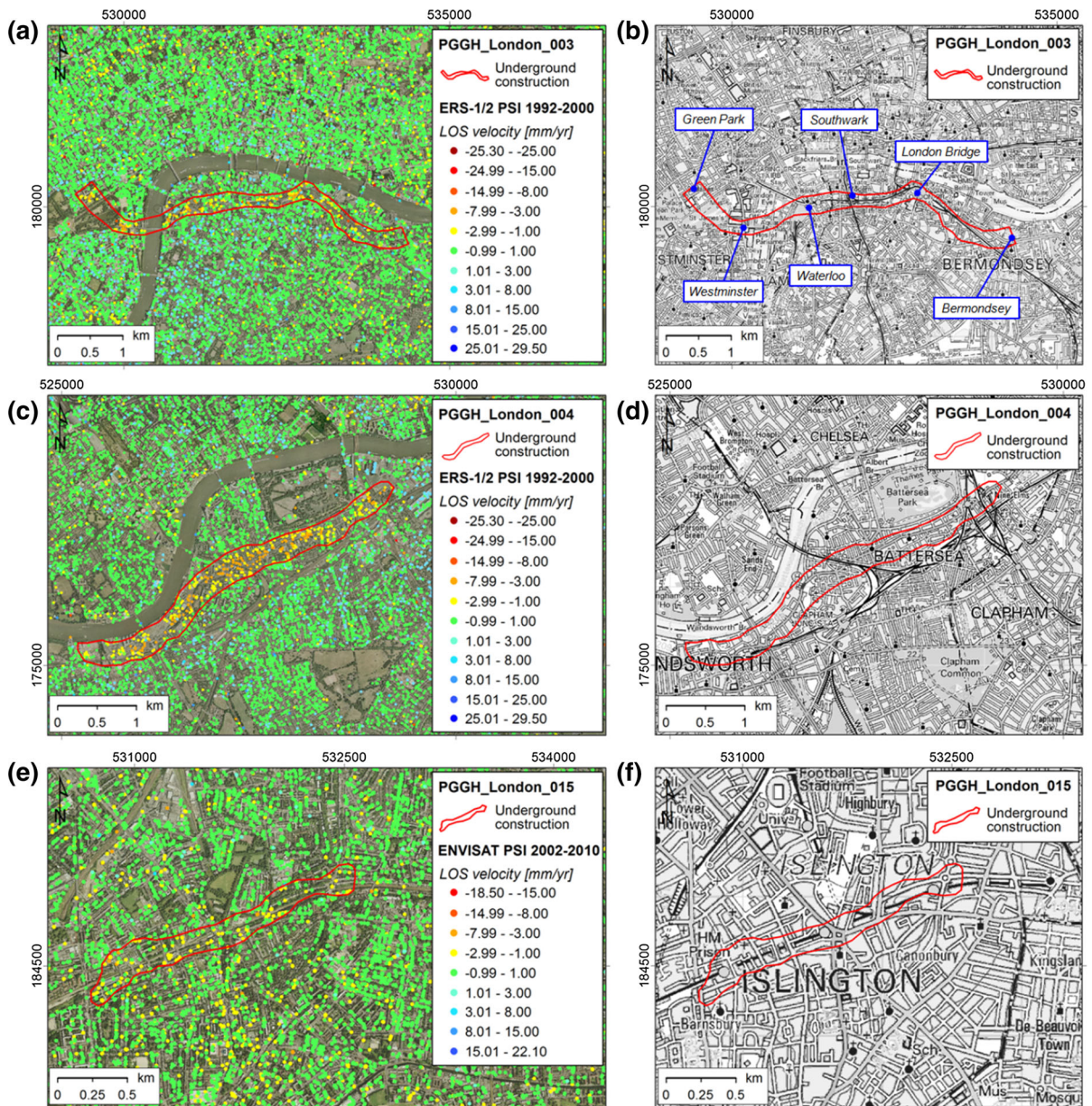


Figure 7

a, c, e Average LOS motion velocities from the ERS-1/2 and ENVISAT PSI results and **b, d, f** OS topographic map at 1:50,000 scale for PanGeo polygons PGGH_London_003 (**a, b**), PGGH_London_004 (**c, d**) and PGGH_London_015 (**e, f**), depicting areas of observed geohazards due to underground constructions in Greater London. PSI data are overlapped onto aerial photographs. Stations of the Jubilee Line Extension track between the stations Green Park and Bermondsey are indicated in **b**. Refer to Table 2 for detailed information and PSI ground motion statistics, and Fig. 3 for location of these polygons within Greater London. British National Grid; Projection: Transverse Mercator; Datum: OSGB 1936. Aerial photography © UKP/Getmapping Licence No. UKP2006/01. OS data © Crown Copyright and database rights 2013

Power, and Queenstown Road Stations, New Covent Garden Market and Wandsworth Bridge. This low-lying area of instability is characterised by deposits of

the Langley Silt Member and Kempton Park Gravel Formation that, towards the centre and south of the polygon, abut Holocene alluvium.

The unstable area coincides with the route of the A3205 between Nine Elms and Wandsworth, along which tunnelling works for electricity cables were carried out between 1997 and 2005 and are the likely cause of the observed ground motion (BINGLEY *et al.* 2007). Observed PS LOS velocity within the geohazard polygon is -1.93 ± 1.78 mm/year from 1992 to 2000, with a peak of -14.0 mm/year achieved by a few isolated PS, corresponding to a movement of -110 mm over the monitored interval (Fig. 7c). Up to -8.0 mm/year are observed in the inner sector of the polygon lying along the axis of the A3205, whereas motion velocity decreases to -1.0 to -3.0 mm/year towards the boundaries of the polygon, with increasing distance from the track of the underground excavation. Our results confirm observations by ALDISS *et al.* (2014), and depict domain '6A' identified by these authors for 1997–2005, as moving at -2.1 ± 1.3 mm/year on average within the domain boundary. Motion velocities estimated by the ENVISAT PS data decrease to -1.81 ± 0.64 mm/year during 2002–2010, and peaks of no more than -6.04 mm/year are observed. During this time period, velocities within the area of PGGH_London_004 are not distinguishable from those affecting the larger surrounding area, and are better attributed to alternative sources of motion (see Sect. 3.2.2).

The third area of underground construction identified by the PSI data extends 0.38 km² within the Islington Borough, and follows the track of the Channel Tunnel Rail Link (CTRL) or High Speed 1 (HS1), the UK high speed rail link between the Channel Tunnel and London St Pancras International, opened in full in November 2007 (cf. 'PGGH_London_015'; Fig. 7e, f; Table 2). The geohazard polygon includes a 2-km long portion of the CTRL tunnel under the built-up areas of London between Caledonian Rd and Barnsbury to the West (before the line emerges on the surface and arrives at St Pancras) and Canonbury to the East, before Stratford station.

Variable motion rates are observed within the polygon area, with most targets moving away from the satellite sensor, and only a few moving towards the sensor. The ERS-1/2 PS data within the geohazard polygon boundary show LOS velocity of -0.07 ± 0.81 mm/year during 1992–2000, whereas

significant acceleration is observed in the ENVISAT data from 2002 to 2010, when values increase to -1.09 ± 0.85 mm/year, with peaks of -5.69 mm/year along the CTRL track (Fig. 7f). We relate the observed motions with ground subsidence resulting from the construction of the track of the CTRL between Caledonian Rd and Barnsbury and Canonbury. Indeed, the above track segment was built during the same time frame of the motions estimated over the ENVISAT data set, and possibly exerted local control on ground stability by inducing compaction of the sediments above the tunnel along its track.

Ground subsidence is also observed over a wider area around this polygon, as revealed by the presence of several PS showing up to -3 mm/year average motion velocities outside the geohazard polygon boundaries (Fig. 7e). This motion is identified by PanGeo polygon 'PGGH_London_006', and is due to groundwater abstraction (see Sect. 3.2.2).

3.2.2 Groundwater Abstraction and Rise

Vast areas of ground motions due to groundwater management are revealed in Greater London by the PSI data and analysis of water level records from the Environment Agency (EA). These concern both areas undergoing land subsidence induced by water pumping and decreased ground water levels in the aquifers, and water rise due to recovery of the historical levels. Ground levels tend to change in response to water levels; for instance, by subsiding when water levels fall, and uplifting when it recovers, as a direct effect of changes in the pore water pressure, and consequently, the effective stress acting on the terrain.

A total of four geohazard polygons belonging to groundwater management are delineated in London, and these are classified as 'Groundwater Abstraction' when showing subsidence, and 'Other' when showing ground uplift.

The wider geohazard polygon relating to this category refers to a large area of 146.65 km², which encompasses portions of 13 London boroughs including those of Islington, City of Westminster, Wandsworth, Lambeth and Southwark, and numerous landmarks such as Hyde Park, St James Palace, the City of Westminster, Wimbledon Common and

London Bridge (cf. ‘PGGH_London_006’; Table 2). Over 80 % of this area is underlain by the London Clay Formation, and the deposits of the Lambeth Group and Thanet Sand Formation are present only in the south-eastern sector. LOS velocity from the PS data within the geohazard polygon boundary reveal -0.81 ± 0.64 mm/year during 2002–2010 and $+0.19 \pm 1.15$ mm/year from 1992 to 2000 for this area, with peak negative (-19.45 mm/year) and positive LOS velocities ($+22.47$ mm/year) achieved in the ERS-1/2 ascending data set. The ENVISAT PSI results display a more consistent trend in ground motion away from the satellite during 2002–2010 (Fig. 8a), and the wide area and range of lithologies over which this negative motion operates suggests a relatively deep-seated cause for the motion.

Monitoring of groundwater levels by the EA (2010) reveals a period of groundwater abstraction within the study area between 2000 and 2010, and a fall in groundwater levels by as much as 22 m has been recorded in the centre of the polygon area (Fig. 8b).

Velocity trends for the PS data from 1992 to 2000 are more variable. A relatively distinct area of positive velocities can be seen centred around Lambeth, and can be attributed to groundwater recharge. This has been delineated as polygon ‘PGGH_London_010’ in PanGeo, and covers a total of 21.29 km² and portions of nine London boroughs, including those of the City of Westminster, Lambeth, Southwark and the City of London. LOS velocity of all the ERS-1/2 PS targets within the polygon is $+0.45 \pm 1.12$ mm/year during 1992–2000 (Fig. 9a),

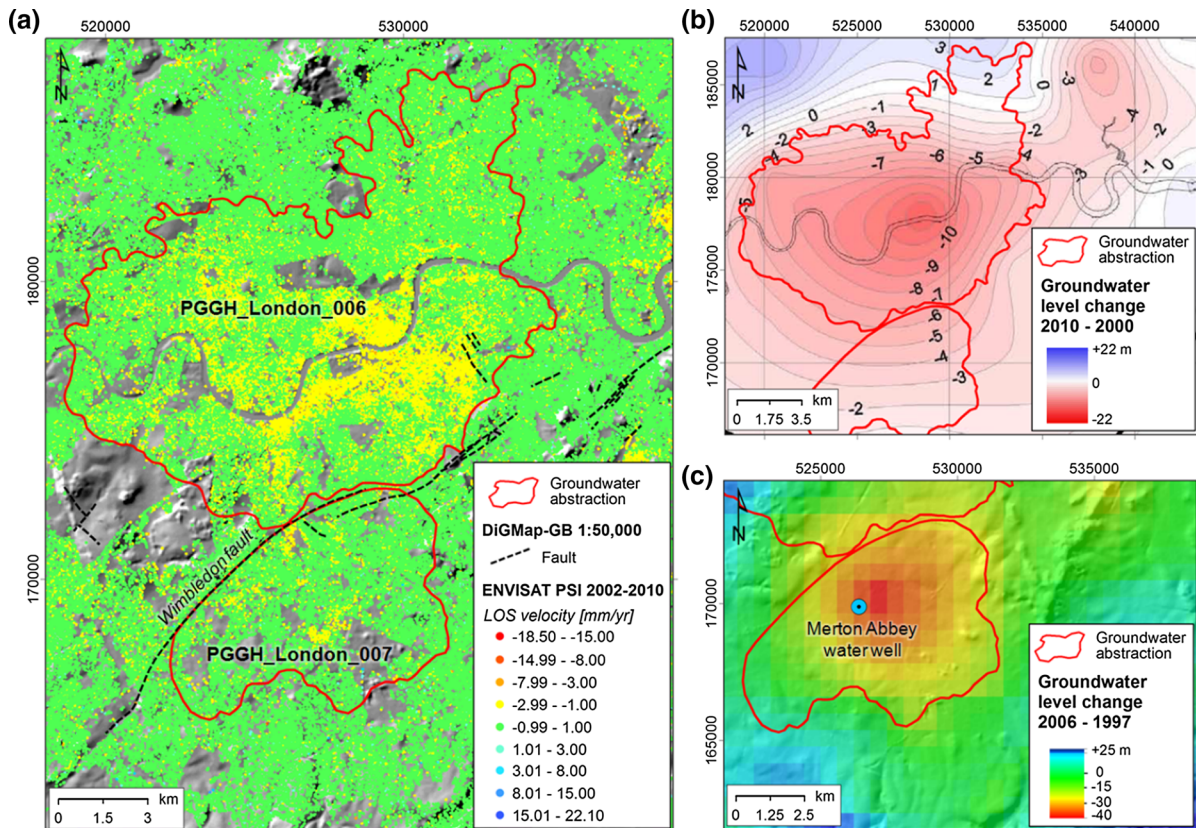


Figure 8

a Faults from the DiGMapGB at 1:50,000 scale and average motion velocities from 2002 to 2010, estimated along the line-of-sight of ENVISAT in descending mode for areas of observed groundwater abstraction; and **b**, **c** groundwater level changes between 2000 and 2010 [modified from EA (2010)] and between 1997 and 2006 [modified from EA (2007)], overlapped onto shaded relief of NEXTMap® DTM at 50 m resolution. Refer to Table 2 for detailed information and PSI ground motion statistics, and Fig. 3 for location of these polygons within Greater London. British National Grid; Projection: Transverse Mercator; Datum: OSGB 1936. Geological materials © NERC, All rights reserved. NEXTMap® Britain © 2003, Intermap Technologies Inc., All rights reserved

with maximum observed velocities of +20.90 mm/year. Monitoring of groundwater levels by the EA (2007) reveals a period of groundwater recharge within the study area between 1996 and 2001 (Fig. 9b). This is particularly the case for the northern section of the polygon area, where values approaching +3.39 m for the period 1997 to 2006 can be seen. Groundwater recharge in these areas facilitates uplift by increasing pore water pressures.

Another area of observed land subsidence due to groundwater abstraction has been delineated and classified as PanGeo polygon 'PGGH_London_007' (Table 2; Fig. 8a, c). This area covers a total of 47.17 km² and includes portions of six Boroughs of Greater London, namely Merton, Sutton, Croydon, Lambeth, Wandsworth and Kingston upon Thames. The bedrock geology of the area is dominated by the London Clay Formation, with small sectors where clays, silt and sand of the Lambeth Group crop out.

Several groundwater wells are located across this geohazard polygon and the observed subsidence is thought to be related to increased ground water abstraction at these locations. Groundwater levels were lowered by 39 m between January 1997 and January 2006 (EA 2007), due to abstraction at the Merton Abbey public water supply well, which is one of a number of sites in this part of the London area where water is taken from the Chalk (i.e., the principal aquifer of the London Basin) at depths in excess of 70 m. Groundwater level maps over 1997–2006 also record rates of groundwater level changes of the order of -2 to -5 m/year from 1996 to 2002.

ERS-1/2 and ENVISAT PS mainly show very low motion rates (in the range ± 1 mm/year) and several zones moving away from the satellite sensor at rates of a few mm/year. LOS velocity of the ERS-1/2 PS within the polygon is -0.14 ± 1.16 mm/year during

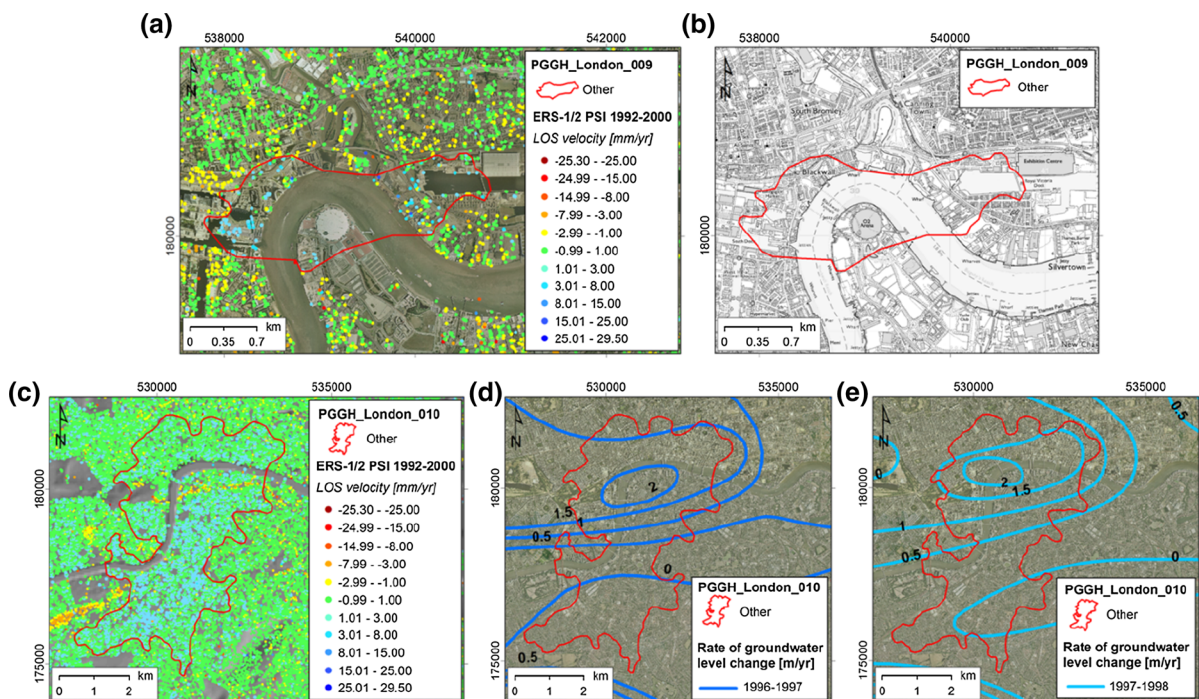


Figure 9

a Average motion velocities from 1992 to 2000, estimated along the line-of-sight of ERS-1/2 in ascending mode, and **b** OS topographic map at 1:25,000 scale for PanGeo polygon PGGH_London_009. **c** Average motion velocities from 1992 to 2000 estimated along the line-of-sight of ERS-1/2 in ascending mode, and **d**, **e** rates of groundwater level change recorded in 1996–1997 and 1997–1998 [modified from EA (2007)]. Refer to Table 2 for detailed information and PSI ground motion statistics, and Fig. 3 for location of these polygons within Greater London. **a**, **d**, and **e** are overlapped onto aerial photographs, whereas **c** onto shaded relief of NEXTMap[®] DTM at 50 m resolution. British National Grid; Projection: Transverse Mercator; Datum: OSGB 1936. Aerial photography © UKP/Getmapping Licence No. UKP2006/01. OS data © Crown Copyright and database rights 2013. NEXTMap[®] Britain © 2003, Intermap Technologies Inc., All rights reserved

1992–2000, with peaks of -25.28 mm/year in the northern sector of the polygon, around Tooting (Fig. 8a). In this area, the fastest water table decrease (-10 m/year) was observed in 2001–2002 (EA 2007). LOS velocity decreases to -0.47 ± 0.62 mm/year in the ENVISAT data from 2002 to 2010 and no more than -8.43 mm/year are observed; however, the areas revealing subsidence in this period appear wider than from 1992 to 2000, and zones moving at higher and consistent rates during 2002–2010 are concentrated in the central sector around Mitcham.

The north-west edge of this geohazard polygon is bounded by the Wimbledon Fault. In this area, it appears that faults parallel to the Wimbledon Fault are exerting control on local subsidence patterns, as major lineaments in average velocity distribution are aligned to these faults (BATESON *et al.* 2009). It is also noteworthy that the width of the Thames floodplain increases markedly downstream of the Wimbledon Fault, as shown by the outcrop of the Holocene deposits. Our PSI data confirm the observations for domain '5A' identified by ALDISS *et al.* (2014), who found velocities of -1.55 ± 0.83 mm/year for this area during 1997–2005, with the largest subsidence rates centred close to the Merton Abbey public water supply well. Ground motions in this area were attributed to groundwater abstraction from the above water well, and were investigated further in the framework of the ESA TerraFirma project, via the production of the TerraFirma—London H3 Modelled Product (BATESON *et al.* 2009). Quantitative analysis and modelling of the relationship between ground motion rates and groundwater pumping from the Merton Abbey water well showed agreement between groundwater modelling results and observed ground motions over the Merton Abbey area.

Lying within the large area of compaction of the Holocene alluvium (see Sect. 3.1.1), land uplift due to groundwater aquifer recharge is also observed for a 2.19 km² area crossing the Tower Hamlets, Greenwich and Newham Boroughs of Greater London, and including the far end of the Greenwich Peninsula in South East London (cf. 'PGGH_London_009'; Table 2). This area is low-lying river flood plain with elevations in the range of 2 to 14 mOD, and maximum values reached in the north-western sector, around Blackwall. The bedrock geology is dominated by the

London Clay Formation and clays, silt and sand of the Lambeth Group, whereas superficial deposits in the area consist mostly of alluvium of the River Thames. Made, infilled and landscaped ground (undivided) is found in this area, and the thickness of the superficial deposits is typically 10–15 m, with maximum values of 30 m in the area of the Blackwall Stairs.

PSI data indicate uplift of the polygon area from 1992 to 2000 with LOS motion rates of $+1.44$ and ± 2.40 mm/year within the geohazard polygon boundary, whereas during the more recent data set of ground motion data from 2002 to 2010, the uplift cannot be distinguished and subsidence is observed with -0.96 ± 1.04 mm/year (Fig. 9c). During 1992–2000 although the PS data show that most of the Canary Wharf area underwent subsidence, the eastern part of that area, around West India Dock and Blackwall Basin underwent uplift and a quite sharp demarcation between uplifting and subsiding ground across the middle of the Canary Wharf area can be observed. Areas of uplift are also seen around the north end of the Blackwall tunnel and extending over to the end of Royal Victoria Dock. The observed ground uplift is thought to be due to groundwater changes during construction of some blocks on Canary Wharf during the late 1980s (e.g., One Canada Square) and associated local disturbance in local water levels. Indeed, to allow the construction works to be performed, the block basements were surrounded by cofferdams, and groundwater level pumped down temporarily. After the construction, ceased groundwater pumping likely resulted in local aquifer recharge and consequent ground uplift.

It is worth noting that despite the urban fabric and presence of radar reflective structures, no PSI points are found over the area of the Millennium Dome in the ERS data set (1992–2000), likely due to significant land cover changes and construction works performed during the 1990s, before the opening of the Dome to the public in 2000 for the Millennium Experience.

3.2.3 Made Ground

Areas undergoing subsidence due to consolidation of artificial ground and compaction of underlying deposits are identified in Greater London and delineated in the geohazard polygons 'PGGH_London_005' and

'PGGH_London_008' (Table 2; Fig. 10). These are both located in the southern sector of the Havering Borough adjacent to the River Thames, and lie within identified geohazard polygon of compressible ground along the flood plain of the River Lea and Thames (see Sect. 3.1.1), in a sector of the Thames flood plain where areas of made ground are largely present.

One of these mapped geohazards is located within the Hornchurch Marshes, and includes the Fairview Industrial Park and car compounds and some business centres along the Marsh, Barlow and Creek Ways. This represents observed ground motion related to subsidence of recent (\sim 1940s) made ground, and covers 1.38 km² low-lying river flood plain with gentle relief and elevations in the range of 2 to 10 mOD. This area is characterised by the presence of the London Clay Formation and the Lambeth Group, which are overlain by alluvium and tidal river or creek deposits. These are generally susceptible to progressive subsidence from compaction, drying and resulting compression.

The geohazard mapped via PanGeo coincides with an area of made ground (undivided), where the thickness of the superficial deposits is between 10 and 25 m (Fig. 10c). For this area, most ERS-1/2 and ENVISAT PS targets show motion away from the satellite sensor, and indicate subsidence in both time intervals 1992–2000 and 2002–2010, with consistent contrast in average velocities between this and adjacent areas. LOS velocity within the polygon is -3.23 ± 3.45 mm/year during 1992–2000, with maximum observed velocities of -15.99 mm/year in the western sector of the polygon area. Velocity decreases to -2.78 ± 2.52 mm/year in the ENVISAT descending data set from 2002 to 2010, and no more than -10.64 mm/year are observed (Fig. 10a, b).

Another similar area of compacting made ground due to the presence of artificial ground (undifferentiated) overlying the Holocene alluvium has been delineated nearby. This covers 0.57 km² and includes sections of the Dagenham motor works and abuts the Dagenham Power Station and Horse Shoe Corner. In this area, the maximum total superficial deposit thickness (including superficial geology and artificial ground) of 21.64 m is reached in the centre of the geohazard polygon (Fig. 10c).

A distinct concentration of PS is visible here when compared to the neighbouring areas, and a significant contribution from the made ground is considered likely with respect to the compaction of the River Thames alluvium, which affects the area at a larger scale. ERS-1/2 and ENVISAT data highlight LOS velocity within the polygon of -1.69 ± 2.38 mm/year during 1992–2000, with maximum observed negative velocities of -11.92 mm/year, and -1.72 ± 1.32 mm/year from 2002 to 2010, with peak velocities of -7.27 mm/year (Table 2; Fig. 10a, b). For this area, the difference in ground motion between other areas of artificial ground within the vicinity is likely due to differing dates of development. For example, the Dagenham Motor Works to the east of the polygon was developed in 1935. Any ground motion related to this older development is, therefore, likely to have slowed with time as the artificial deposits settle.

3.3. Unknown Geohazards

A number of areas showing ground motion but with a level of uncertainty in their related causes was observed (cf. 'Unknown' hazard types in Table 2). For these geohazard polygons, although clear spatial evidence of the presence of land motion was revealed by the PSI data, it was difficult to attribute with confidence a type or category due to the absence of validation with external data or information.

Geohazards of unknown origin and cause are, for instance, found in north-west London in the Harrow, Barnet and Brent Boroughs. At the intersection of the latter, 11 km north of the River Thames, a narrow 0.44 km² polygon following the line of the Edgware Road (A5) from junction with B461 to Annesley Avenue for a total of 2.39 km is observed (cf. 'PGGH_London_018'; Fig. 11a). Subsidence is clearly visible between 2002 and 2010, and LOS velocity is -1.10 ± 0.66 mm/year in the ENVISAT data set, with peak of -3.59 mm/year. Given the close association with the local transport network and concentrated temporal nature of the motion, the cause is likely to be anthropogenic activity in the area. As the area is underlain by the London Clay Formation, which is a known shrink–swell-prone lithology, altered drainage during 2002–2010 may be a possible

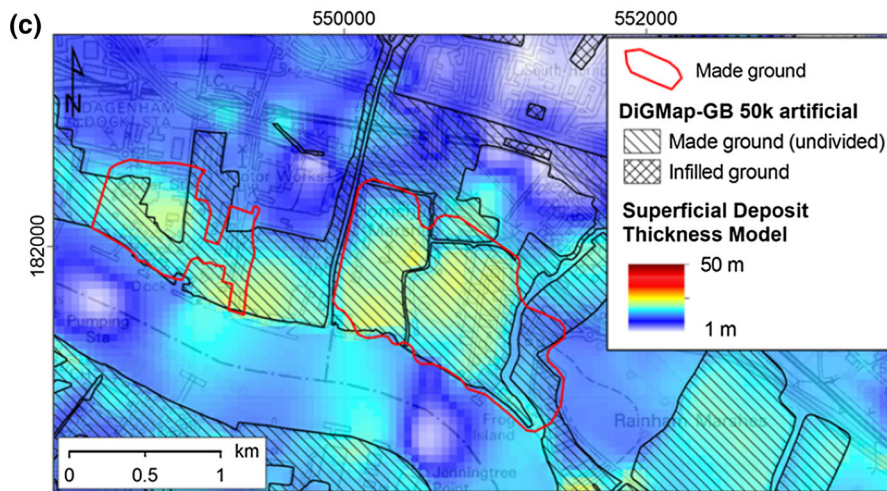
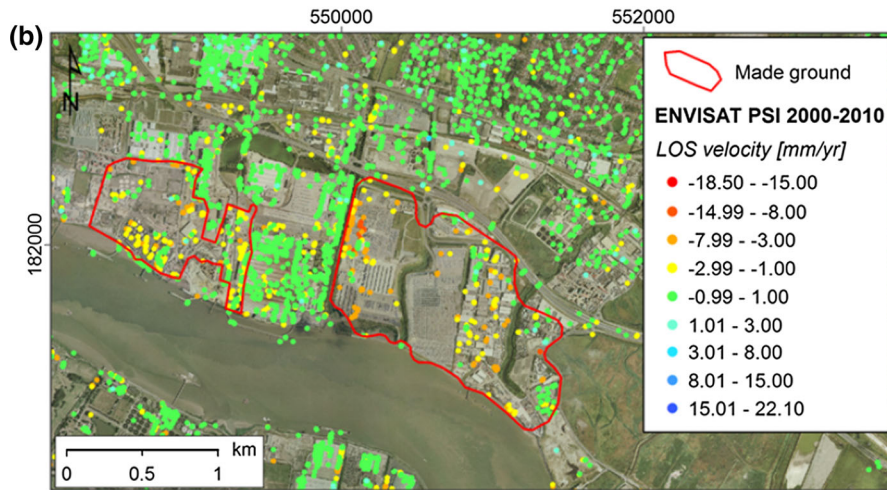
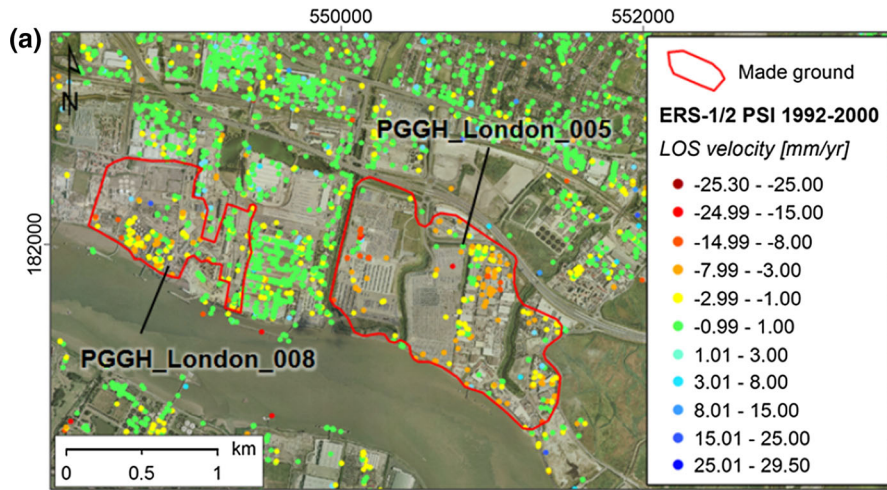


Figure 10

Average motion velocities from 1992 to 2000 (a) and from 2002 to 2010 (b), estimated along the line-of-sight of ERS-1/2 in ascending mode and ENVISAT descending mode, respectively, overlapped onto aerial photographs, for areas of observed made ground in Greater London. c Artificial deposits from BGS DiGMapGB at 1:50,000 scale, onto Superficial Deposit Thicknesses derived from the BGS Superficial Deposit Thickness Model (SDTM) and OS topographic map at 1:50,000 scale. Refer to Table 2 for detailed information and PSI ground motion statistics, and Fig. 3 for location of these polygons within Greater London. British National Grid; Projection: Transverse Mercator; Datum: OSGB 1936. Aerial photography © UKP/Getmapping Licence No UKP2006/01. OS data © Crown Copyright and database rights 2013

cause. In this instance, the improvement of drainage from the road network or improved buried utilities will reduce water leaks and consequent swell of the underlying clay, though no direct proof of this hypothesis is available.

To the north-west of this area, another small area of observed ground motions is found (cf. 'PGGH_London_017'; Fig. 11b). This coincides with the Staples Corner, a major road junction of London built in the 1960s and consisting of two linked roundabouts and flyovers that connect the A406/North Circular Road (crossing North London, and linking W and E London) with the A5 Edgware Road, and the start of the M1 motorway. LOS velocity of the PS data within the polygon was -0.85 ± 1.67 mm/year during 1992–2000, and -1.33 ± 1.17 mm/year during 2002–2010. ERS-1/2 PS moving at -3.3 to -3.7 mm/year from 1992 to 2000 are found over the A406 flyover, and at up to -9.1 mm/year over the JVC, London Group and Aquarius Business Parks (north of the A406/North Circular Road). ENVISAT data show more consistently distributed motions all over the geohazard polygon, and up to -3.0 mm/year of along the infrastructure of the roundabout to the M1 and the business parks north of the A406/North Circular Road, and -3.4 mm/year along the A5 Edgware Road.

Serious damage to the road infrastructure and nearby buildings was caused by the explosion of a Provisional IRA van bomb underneath the A406 flyover and near the junction in the early 1990s, and the junction was temporarily closed for reconstruction and repair works. The format of the junction was modified during the reconstruction works and an additional slip road onto the M1 from the east

was added. Although no definite causative relationship of the observed ground motions was identified for this polygon, it is worth considering a possible correlation with these events. Indeed, the engineering works for the reconstruction and repairing of the junction might have been followed by structural and ground settlement that was imaged by the satellite data.

Another area of ground motion with unknown causes is centred on the Sloane Sq. London Underground station, which is served by the District and Circle Lines and is between South Kensington and Victoria (cf. 'PGGH_London_011'; Fig. 11c). This area is generally low-lying with elevations in the range of 11 to 16 mOD, and lies over alluvium and sediments of the River Westbourne that ran southwards towards the Thames through Hyde Park as the Serpentine Lake, and originally crossed by the Knight's Bridge at Knightsbridge. At Sloane Sq., the River Westbourne now flows over the Circle and District Line platforms inside a large iron conduit suspended from girders that was built in the 1850s when Belgravia, Chelsea and Paddington were developed. PS data indicating a general pattern of subsidence within this area during 1992–2010, with LOS velocity of -1.34 ± 0.37 mm/year during 1992–2000, and -1.74 ± 0.63 mm/year during 2002–2010. This area corresponds with domain '6B' identified by ALDISS *et al.* (2014), who estimated up to -5.1 mm/year at the centre of the unstable area. Historical records document groundwater flood incidents due to heavy rainfall and sewer surcharge occurred in 2006 and 2007 in the Sloane Sq. and the Notting Hill London Underground stations (HALCROW 2011), and preliminary Flood Risk Assessments and Flood Risk Areas for the Royal Borough of Kensington and Chelsea from EA indicate widespread vulnerability to surface water flooding across the entire Borough. Although for Sloane Sq. the extension of the critical drainage area coincides approximately with the location of the observed ground motions, no direct correlation between the latter and the above events has been identified.

Details and PSI observations for all unknown geohazards found in Greater London are discussed within the GHD report for London, i.e., CIGNA *et al.* (2013c).

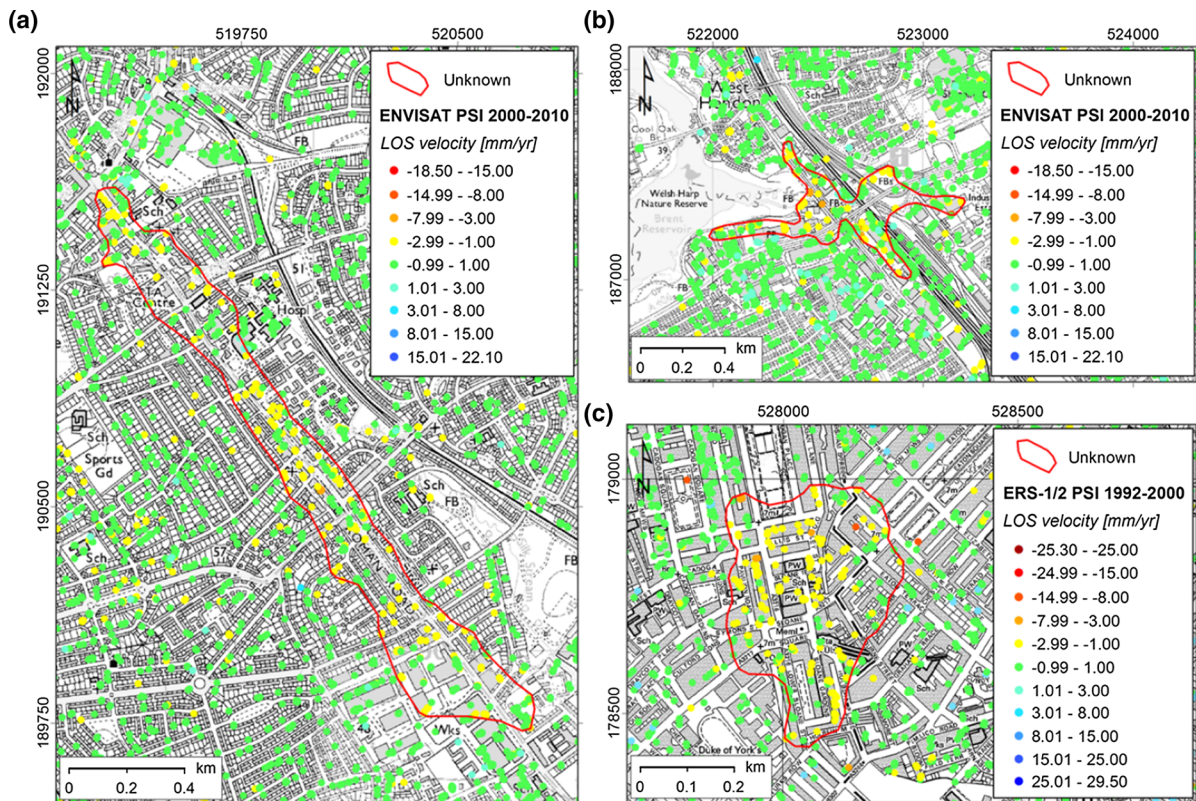


Figure 11

Examples of observed geohazards of unknown category in Greater London: PanGeo polygons **a** PGGH_London_018, **b** PGGH_London_017, and **c** PGGH_London_011. Average motion velocities in **a**, **b** 2002–2010 and **c** 1992–2000 estimated along the lines-of-sight of ENVISAT descending mode and ERS-1/2 in ascending mode, respectively. PSI data are overlapped onto OS topographic maps at **a**, **b** 1:25,000 and **c** 1:10,000 scales. Refer to Table 2 for detailed information and PSI ground motion statistics, and Fig. 3 for location of these polygons within Greater London. British National Grid; Projection: Transverse Mercator; Datum: OSGB 1936. OS data © Crown Copyright and database rights 2013

3.4. Discussion

PSI ground motion data for Greater London help to place the capabilities of these remote sensing techniques into a wider context, and analyse their potential to detect surface motions related to near-surface geological processes and the surface expression of deeper-seated motions and dynamics.

From the typologies of ground motions that we were able to detect and delineate with confidence using PSI, it becomes apparent that InSAR and PSI with such input as ERS and ENVISAT SAR data are generally sensitive to slow (up to a few tens of mm/year), relatively constant through time, ground motions, such as compressible ground and the effects of ground water abstraction and rise. For instance, we

observe in Greater London what we expected along the River Thames and other flood plains (see Sect. 3.1.1), and the consequences of groundwater level changes in the main aquifer are also evident across the investigated area (see Sect. 3.2.2). There are, however, geohazards that affect London for which the PSI data encountered difficulties in depicting.

It has been observed and largely discussed that Palaeogene clays of the London Clay and Lambeth Group and other Mesozoic and Tertiary clay soils and mudrocks are susceptible to natural shrinkage and swelling induced by variations in moisture content induced by changes in environmental conditions (e.g., HARRISON *et al.* 2012; JONES and JEFFERSON

2012). This type of geohazard has not been identified via the interpretation of average ground motion velocities from the PSI data for Greater London. We believe that this is partly due to the difficulties of the ERS-1/2 and ENVISAT PSI data in distinguishing the generally low rates of motion associated with long-term shrinkage (e.g., HOBBS *et al.* 2014; and references therein) with respect to other land processes that occur over vast areas (e.g., compaction of alluvium). Moreover, the usually seasonally variable motion history of shrinkage and swelling clays cannot clearly be highlighted by the interpretation of the sole average motion velocities. Indeed, detailed analysis of single PS time series would be required to verify whether such seasonal variations are depicted by the PSI data, but such an analysis by visual inspection for more than hundreds of thousands of targets is unfeasible. A few studies have tried to overcome this limitation and to ease the task of the radar interpreters to identify nonlinear components within large volumes of PSI data sets (BERTI *et al.* 2013; CIGNA *et al.* 2012b; TAPETE and CASAGLI 2013). These approaches will be tested and assessed with our data in Greater London to verify whether observed geohazards relating to shrink–swell clays can be incorporated into upgraded version of the PanGeo product.

Another geohazard that is apparently missed by the PSI data concerns dissolution processes. Although this geohazard has been both observed in the field and recorded in the National Karst Database (FARRANT and COOPER 2008) and in terms of susceptibility via the GeoSure data set, for instance where the white Cretaceous Chalk is present in the southern sector of Greater London, no PanGeo polygons are associated to this particular geohazard. This is due to the fact that dissolution processes and associated motions are generally faster than the maximum potential motion that PSI techniques can estimate before encountering phase unwrapping problems (i.e., 15 cm/year for ERS or ENVISAT data with 35 days repeat cycle). As of today, only in a few cases InSAR-based studies have been successful to image land motions associated with karstic features, and these mainly relate to conventional InSAR applications, and only in a few instances to multi-interferogram techniques (e.g., CASTAÑEDA *et al.* 2009; CLOSSON *et al.* 2005; FERRETTI

et al. 2004; GUTIÉRREZ *et al.* 2011), to the best of our knowledge.

With regard to landsliding, very few PS targets were found across the investigated area within the mapped landslide deposits or in close proximity to landslide deposits as mapped in the DiGMapGB. This evidence can be mostly explained by analysing the typical land covers of landslide deposits in Greater London, which mainly shows green urban areas, forests and agricultural land covers, and only in a few instances, small areas of urban fabric of generally low density [cf. also CIGNA *et al.* (2013c)]. These land cover types are generally affected by significant temporal decorrelation and strong variations of the interferometric phase, which prevent good radar reflectors to be identified within the radar imagery stacks (e.g., CIGNA *et al.* 2013a, b; COLESANTI and WASOWSKI 2006). Rapid ground motions are a further possible explanation for low PS density; however, we believe that this factor does not play a role for the landslide processes mapped within Greater London, due to their age and recent state of inactivity as mapped in the database and geological maps (see Sect. 3.1.2). The state of inactivity of these landslides also results in the absence of apparent evidence of surface motion in the PSI data for the majority of the mapped landslide deposits in Greater London. These often refer to inactive (e.g., stabilized or relict) phenomena that are depicted by the PSI average velocities as stable or undergoing almost null motions [cf. also CIGNA *et al.* (2013c)].

The identification of geohazards for the generation of the PanGeo products was, for Greater London, largely focussed on EO data and the analysis of PSI ground motion data that covers the period 1992–2010. Therefore, the products and polygons do not claim to be an exhaustive representation of all geohazards affecting the administrative area. This is mainly due to the temporal coverage of the PSI data sets that can only look as far back as the SAR archive data allows (to the beginning of the 1990s).

Further need to integrate the PanGeo geohazards products is found in the representation of areas susceptible to the various geohazards, where ground motions are potential, but have not necessarily occurred. As mentioned above, geohazard susceptibility mapping has been undertaken by the BGS for

the entire landmass of Great Britain, and is available through the BGS's commercial GeoSure data set (BOOTH *et al.* 2010; WALSBY 2008). Thus, the use of the PanGeo GSL for Greater London in conjunction with areas of potential geohazards identified through GeoSure is highly recommended.

4. Conclusions

We have mapped a range of interacting natural and manmade geohazards within the administrative area of Greater London, by combining ground motion data derived from the IPTA processing of ERS-1/2 and ENVISAT SAR images acquired between 1992 and 2010, with a variety of geological and other geospatial layers.

Areas of observed geohazards that were identified via the PanGeo standardised methodology cover a total of over 40 % of the investigated area (i.e., $\sim 650 \text{ km}^2$ out of a total of $\sim 1,580 \text{ km}^2$), and range from natural compaction of the Holocene deposits of the River Thames flood plain, to land subsidence and heave resulting from groundwater management for engineering works or domestic use, and changes in the groundwater levels in the main aquifer of the London Basin. Observed ground motions indicate a combination of land surface processes comprising ground subsidence and uplift, as well as down slope movements, and minimum and maximum observed LOS velocities are -25.3 and $+29.5$ mm/year during 1992–2010.

Integration of the geohazard mapping with the Copernicus EEA European Urban Atlas has revealed greater spatial variability of observed motion velocities within non-urban land cover types such as agricultural, semi-natural and green areas, when compared to observations for continuous and discontinuous urban fabric and industrial units that seem to show the smallest standard deviations in their annual velocity statistics.

We have also analysed difficulties in the identification of land processes relating to the shrink–swell of clayey deposits that are based mainly upon interpreting just the velocity and not the time series spatio-temporally, and to ground dissolution and collapse, the associated difficulties of which mainly

relate to technological constraints due to temporal decorrelation. Challenges relating to the detection of good radar targets for PSI analysis in landsliding affected rural areas are also discussed. Future research will focus on analysing further PSI data for this area with specific regard to these geohazards; for instance, to ascertain whether seasonal variations of ground levels due to shrinking–swelling clays have been depicted by the motion time series of the radar targets identified across Greater London, or to verify whether precursors of ground collapses have been recorded by the PSI data in areas subject to dissolution processes. Further research is already being carried out at BGS to test and assess new processing techniques to improve the radar target coverage and density in non-urban areas. The latter has been recognized as a priority for areas like the UK, where land cover exerts significant control on the success of interferometric studies using C-band SAR imagery (BATESON *et al.* 2014; CIGNA *et al.* 2013a, 2014).

Acknowledgments

The research leading to these results has received funding from the European Union's Seventh Framework Programme (FP7/2007–2013) under grant agreement no. 262371. The authors would like to thank Ren Capes, formerly PanGeo Project Coordinator at CGG—NPA Satellite Mapping, for launching, leading and promoting the project with dedication from 2011 to 2013, and Prof. Stuart Marsh, formerly at BGS, for chairing the Service Design and Validation Panel in PanGeo and his enthusiastic contribution to the project. Lee Jones at BGS is acknowledged for his support with the discussion on expansive soils, and Don Aldiss, formerly at BGS, for aspects concerning local geology of the London area. F. Cigna, H. Jordan and L. Bateson publish with the permission of the Executive Director of the British Geological Survey (BGS), Natural Environment Research Council (NERC). PanGeo Data: Copyright © 2012. Used and/or reproduced with the permission of the rights holders who participated in the EC FP7 PanGeo Project (262371) and European Environment Agency. Details of the rights holders and the terms of the

licence to use PanGeo project data can be found at <http://www.pangeoproject.eu>. Ordnance Survey data © Crown Copyright and database rights 2013. Geological materials © NERC, All rights reserved. GMES EEA Urban Atlas © EEA 2013, Directorate-General Enterprise and Industry (DG-ENTR), Directorate-General for Regional Policy. NEXT-Map® Britain © 2003, Intermap Technologies Inc., All rights reserved. Aerial photography © UKP/Getmapping Licence No. UKP2006/01.

Open Access This article is distributed under the terms of the Creative Commons Attribution License which permits any use, distribution, and reproduction in any medium, provided the original author(s) and the source are credited.

REFERENCES

- ALDISS, D., BURKE, H., CHACKSFIELD, B., BINGLEY, R., TEFERLE, N., WILLIAMS, S., BLACKMAN, D., BURREN, R. and PRESS, N., 2014. *Geological interpretation of current subsidence and uplift in the London area, UK, as shown by high precision satellite-based surveying*. Proceedings of the Geologists' Association, 125(1): 1–13.
- AMELUNG, F., GALLOWAY, D.L., BELL, J.W., ZEBKER, H.A. and LACZNAK, R.J., 1999. *Sensing the ups and downs of Las Vegas: InSAR reveals structural control of land subsidence and aquifer-system deformation*. Geology, 27(6): 483–486.
- ASTRIUM-GEO, 2014. Underground Construction in Budapest: TerraSAR-X-based analysis of surface movement phenomena related to underground construction in Budapest Available at: <http://www.astrium-geo.com/en/140-underground-construction-in-budapest>, Accessed on: 07/03/2014.
- BANTON, C., BATESON, L., MCCORMACK, H., HOLLEY, R., WATSON, I., BURREN, R., LAWRENCE, D. and CIGNA, F., 2013. Monitoring post-closure large scale surface deformation in mining areas, Mine Closure 2013, Eighth International Conference on Mine Closure. Australian Centre for Geomechanics, Perth, Eden Project, Cornwall, UK.
- BATESON, L., 2013. PanGeo—D3.3 Product and Service Specification. Version 2.3, 51 pp. Available at: [http://www.pangeoproject.eu/sites/default/files/pangeo_other/D3.3-Product-Specification-v1-of-4th-Aug-2011\[1\].pdf](http://www.pangeoproject.eu/sites/default/files/pangeo_other/D3.3-Product-Specification-v1-of-4th-Aug-2011[1].pdf). Accessed on: 30/06/2014.
- BATESON, L., CIGNA, F., BOON, D. and SOWTER, A., 2014. The application of the Intermittent SBAS (ISBAS) InSAR method to the South Wales Coalfield, UK. International Journal of Applied Earth Observation and Geoinformation 34:249–257.
- BATESON, L., CUEVAS, M., CROSETTO, M., CIGNA, F., SCHIJF, M. and EVANS, H., 2012. PANGEO: enabling access to geological information in support of GMES: deliverable 3.5 production manual. Version 1. Available at: http://www.pangeoproject.eu/sites/default/files/pangeo_other/D3.5-PanGeo-Production-Manual-v1.3.pdf. Accessed on: 07/03/2014.
- BATESON, L.B., BARKWITH, A.K.A.P., HUGHES, A.G. and ALDISS, D., 2009. Terraforma: London H-3 Modelled Product. Comparison of PS data with the results of a groundwater abstraction related subsidence Model. British Geological Survey Commissioned Report, OR/09/032, 47 pp.
- BECKEN, K.H. and GREEN, C.A., 2000. *DiGMap: a digital geological map of the United Kingdom*. Earthwise, 16:8–9.
- BELL, J.W., AMELUNG, F., FERRETTI, A., BIANCHI, M. and NOVALLI, F., 2008. *Permanent scatterer InSAR reveals seasonal and long-term aquifer-system response to groundwater pumping and artificial recharge*. Water Resources Research, 44(2):W02407.
- BERARDINO, P., FORNARO, G., FRANCESCHETTI, G., LANARI, R., SANOSTI, E. and TESAURO, M., 2000. Subsidence effects inside the city of Napoli (Italy) revealed by differential SAR interferometry, Geoscience and Remote Sensing Symposium, 2000. Proceedings. IGARSS 2000. IEEE 2000 International, pp. 2765–2767 vol.6.
- BERTI, M., CORSINI, A., FRANCESCHINI, S. and IANNAcone, J.P., 2013. *Automated classification of Persistent Scatterers Interferometry time series*. Nat. Hazards Earth Syst. Sci., 13(8): 1945–1958.
- BGS, 2014. GeoSure: National Ground Stability Data. Available at: <http://www.bgs.ac.uk/products/geosure/home.html>, Accessed on: 07/03/2014.
- BINGLEY, R., TEFERLE, F.N., ORLIAC, E.J., DODSON, A.H., WILLIAMS, S.D.P., BLACKMAN, D.L., BAKER, T.F., RIEDMANN, M., HAYNES, M., ALDISS, D.T., BURKE, H.C., CHACKSFIELD, B.C. and TRAGHEIM, D.G., 2007. Absolute Fixing of Tide Gauge Benchmarks and Land Levels: Measuring Changes in Land and Sea Levels around the coast of Great Britain and along the Thames Estuary and River Thames using GPS, Absolute Gravimetry, Persistent Scatterer Interferometry and Tide Gauges. Joint DEFRA/EA Flood and Coastal Erosion Risk Management R&D Programme. Available at: <http://nora.nerc.ac.uk/1493/1/Absolutefixing.pdf>, Accessed on: 07/03/2014.
- BOOTH, K.A., DIAZ DOCE, D., HARRISON, M. and WILDMAN, G., 2010. User Guide for the British Geological Survey GeoSure data set. British Geological Survey Internal Report, OR/10/066, 17 pp.
- BURLAND, J.B., STANDING, J.R. and JARDINE, F.M., 2001. Building response to tunnelling: Case studies from the construction of the Jubilee Line Extension, London. Volume 1: projects and methods.
- CASTAÑEDA, C., GUTIÉRREZ, F., MANUNTA, M. and GALVE, J.P., 2009. *DInSAR measurements of ground deformation by sinkholes, mining subsidence, and landslides, Ebro River, Spain*. Earth Surface Processes and Landforms, 34(11): 1562–1574.
- CIGNA, F., BATESON, L., JORDAN, C. and DASHWOOD, C., 2013a. Nationwide monitoring of geohazards in Great Britain with InSAR: Feasibility mapping based on ERS-1/2 and ENVISAT imagery. 2013 IEEE International Geoscience and Remote Sensing Symposium (IGARSS 2013), pp. 672–675.
- CIGNA, F., BATESON, L., JORDAN, C. and DASHWOOD, C., 2014. *Simulating SAR geometric distortions and predicting Persistent Scatterer densities for ERS-1/2 and ENVISAT C-band SAR and InSAR applications: nationwide feasibility assessment to monitor the landmass of Great Britain with SAR imagery*. Remote Sensing of Environment, 152, 441–466, doi:10.1016/j.rse.2014.06.025.
- CIGNA, F., BIANCHINI, S. and CASAGLI, N., 2013b. *How to assess landslide activity and intensity with Persistent Scatterer Interferometry (PSI): The PSI-based matrix approach*. Landslides, 10(3): 267–283.
- CIGNA, F., JORDAN, H. and BATESON, L., 2013c. GeoHazard Description for London, Version 2.0. Available at: <http://www.pangeoproject.eu/pdfs/english/London/Geohazard-Description-london.pdf>, 194 pp. Accessed on: 07/03/2014.

- CIGNA, F., OSMANOĞLU, B., CABRAL-CANO, E., DIXON, T.H., ÁVILA-OLIVERA, J.A., GARDUÑO-MONROY, V.H., DEMETS, C. and WDO- WINSKI, S., 2012a. *Monitoring land subsidence and its induced geological hazard with Synthetic Aperture Radar Interferometry: a case study in Morelia, Mexico*. *Remote Sensing of Environment*, 117: 146–161.
- CIGNA, F., TAPETE, D. and CASAGLI, N., 2012b. *Semi-automated extraction of Deviation Indexes (DI) from satellite Persistent Scatterers time series: tests on sedimentary volcanism and tectonically-induced motions*. *Nonlin. Processes Geophys*, 19: 643–655.
- CLOSSON, D., KARAKI, N.A., KLINGER, Y. and HUSSEIN, M.J., 2005. *Subsidence and sinkhole hazard assessment in the Southern Dead Sea area, Jordan*. *Pure and Applied Geophysics*, 162(2): 221–248.
- COLESANTI, C. and WASOWSKI, J., 2006. *Investigating landslides with space-borne Synthetic Aperture Radar (SAR) interferometry*. *Engineering Geology*, 88(3–4): 173–199.
- COOPER, A.H., FARRANT, A.R. and PRICE, S.J., 2011. *The use of karst geomorphology for planning, hazard avoidance and development in Great Britain*. *Geomorphology*, 134(1–2): 118–131.
- CROSETTO, M., MONSERRAT, O., ADAM, N., PARIZZI, A., BREMMER, C., DORTLAND, S., HANSEN, R.F., & VAN LEIJEN, F.J. (2008). Validation of existing processing chains in TerraFirma stage 2—Final Report. GMES TERRAFIRMA ESRIN/Contract no. 19366/05/I-E. (15 pp.).
- CROSETTO, M., MONSERRAT, O., IGLESIAS, R. and CRIPPA, B., 2010. *Persistent Scatterer Interferometry: Potential, Limits and Initial C- and X-band Comparison*. *Photogrammetric Engineering and Remote Sensing*, 76(9): 1061–1069.
- CULSHAW, M., TRAGHEIM, D., BATESON, L. and DONNELLY, L., 2006. Measurement of ground movements in Stoke-on-Trent (UK) using radar interferometry. In: M. Culshaw, H. Reeves, I. Jefferson and T. Spink (Editors), 10th Congress of the International Association for Engineering Geology and the Environment, IAEG2006. Geological Society, London, Nottingham, UK, pp. 1–10.
- EA, 2007. Groundwater Levels in the Chalk-Basal Sands Aquifer of the London Basin. Unpublished report.
- EA, 2010. Management of the London Basin Chalk Aquifer. Status Report 2010. Environment Agency of England and Wales, Thames Region Report.
- EC-JRC, 2013. D2.8.III.12 Data Specification on Natural Risk Zones— Technical Guidelines. Available at: http://inspire.jrc.ec.europa.eu/documents/Data_Specifications/INSPIRE_DataSpecification_NZ_v3.0.pdf, Accessed on: 07/03/2014.
- EC, 2011. Mapping Guide for a European Urban Atlas. Available at: <http://www.eea.europa.eu/data-and-maps/data/urban-atlas/>, 31 pp. Accessed on: 07/03/2014.
- ELLISON, R.A., WOODS, M.A., ALLEN, D.J., FORSTER, A., PHAROAH, T.C. and KING, C., 2004. *Geology of London*. Memoir of the British Geological Survey, Sheets 256 (North London), 257 (Romford), 270 (South London), 271 (Dartford) (England and Wales). 114 pp.
- ESA, 2009. The TerraFirma Atlas. Terrain-motion across Europe. A compendium of results produced by the European Space Agency GMES service element project TerraFirma 2003–2009. Available at: <http://esamultimedia.esa.int/multimedia/publications/TerraFirmaAtlas/pageflip.html>, 94 pp. Accessed on: 07/03/2014.
- EVANS, H., PENNINGTON, C., JORDAN, C. and FOSTER, C., 2013. Mapping a Nation's Landslides: A Novel Multi-Stage Methodology. In: C. Margottini, P. Canuti and K. Sassa (Editors), *Landslide Science and Practice*. Springer Berlin Heidelberg, pp. 21–27.
- FARRANT, A.R. and COOPER, A.H., 2008. *Karst geohazards in the UK: the use of digital data for hazard management*. *Quarterly Journal of Engineering Geology and Hydrogeology*, 41(3): 339–356.
- FERRETTI, A., BASILICO, M., NOVALI, F. and PRATI, C., 2004. Possibile utilizzo di dati radar satellitari per individuazione e monitoraggio di fenomeni di sinkholes. In: S. Nisio, S. Panetta and L. Vita (Editors), *Stato dell'arte sullo studio dei fenomeni di sinkholes e ruolo delle amministrazioni statali e locali nel governo del territorio*, APAT, Roma (2004), pp. 331–340.
- FORSTER, A., 1997. The Engineering Geology of the London Area 1:50,000 Geological sheets 256, 257, 270, 271. British Geological Survey Technical Report WN/97/27.
- FORSTER, A., WILDMAN, G. and POULTON, C., 2003. Landslide potential modelling of North London. British Geological Survey Internal Report. IR/03/122R.
- FOSTER, C., PENNINGTON, C.V.L., CULSHAW, M.G. and LAWRIE, K., 2012. *The national landslide database of Great Britain: development, evolution and applications*. *Environmental Earth Sciences*, 66(3): 941–953.
- GALLOWAY, D.L., HUDNUT, K.W., INGEBRITSEN, S.E., PHILLIPS, S.P., PELTZER, G., ROGEZ, F. and ROSEN, P.A., 1998. *Detection of aquifer system compaction and land subsidence using interferometric synthetic aperture radar, Antelope Valley, Mojave Desert, California*. *Water Resources Research*, 34(10): 2573–2585.
- GIBSON, A.D., CULSHAW, M.G., DASHWOOD, C. and PENNINGTON, C.V.L., 2013. *Landslide management in the UK—the problem of managing hazards in a 'low-risk' environment*. *Landslides*, 10(5): 599–610.
- GIGLI, G., FRODELLA, W., MUGNAI, F., TAPETE, D., CIGNA, F., FANTI, R., INTRIERI, E. and LOMBARDI, L., 2012. *Instability mechanisms affecting cultural heritage sites in the Maltese Archipelago*. *Natural Hazards and Earth System Sciences*, 12(6): 1883–1903.
- GUTIÉRREZ, F., GALVE, J.P., LUCHA, P., CASTAÑEDA, C., BONACHEA, J. and GUERRERO, J., 2011. *Integrating geomorphological mapping, trenching, InSAR and GPR for the identification and characterization of sinkholes: A review and application in the mantled evaporite karst of the Ebro Valley (NE Spain)*. *Geomorphology*, 134(1–2): 144–156.
- HALCROW, 2011. Surface Water Management Plan for Royal Borough of Kensington & Chelsea, Drain London. The Royal Borough of Kensington and Chelsea. SWMP Halcrow Report for RBKC, v0.10. Aug 2011.
- HANSEN, R.F., VAN LEIJEN, F.J., VAN ZWIETEN, G.J., BREMMER, C., DORTLAND, S. and KLEUSKENS, M., 2008. Validation of existing processing chains in TerraFirma stage 2. Product validation: validation in the Amsterdam and Alkmaar area. TerraFirma project report. Accessed on: 26/05/2008.
- HARRISON, A.M., PLIM, J.F.M., HARRISON, M., JONES, L.D. and CULSHAW, M.G., 2012. *The relationship between shrink–swell occurrence and climate in south-east England*. *Proceedings of the Geologists' Association*, 123(4): 556–575.
- HERRERA, G., FERNÁNDEZ, J.A., TOMÁS, R., COOKSLEY, G. and MULAS, J., 2009. *Advanced interpretation of subsidence in Murcia (SE Spain) using A-DInSAR data—modelling and validation*. *Nat. Hazards Earth Syst. Sci.*, 9(3): 647–661.
- HOBBS, P.R.N., JONES, L.D., KIRKHAM, M.P., ROBERTS, P., HASLAM, E.P. and GUNN, D.A., 2014. *A new apparatus for determining the shrinkage limit of clay soils*, *Géotechnique*, 64(3): 195–203.

- JONES, L.D. and JEFFERSON, I., 2012. Expansive soils. In: J. Burland, T. Chapman, H. Skinner and M. Brown (Editors), ICE Manual of Geotechnical Engineering. Volume 1: Geotechnical Engineering Principles, Problematic Soils and Site Investigation. ICE Publishing, London, UK, pp. 413–441.
- JONES, L.D. and TERRINGTON, R., 2011. *Modelling Volume Change Potential in the London Clay*. Quarterly Journal of Engineering Geology and Hydrogeology, 44(1): 109–122.
- JORDAN, H., CIGNA, F. and BATESON, L., 2013. GeoHazard Description for Stoke-On-Trent, Version 1.0. Available at: <http://www.pangeoproject.eu/pdfs/english/stoke/Geohazard-Description-stoke.pdf>, 122 pp. Accessed on: 07/03/2014.
- KRIVENKO, A., RIEDEL, B., NIEMEIER, W., SCHINDLER, S., HECK, P., MARK, P. and ZIEM, E., 2012. Application of Radar Interferometry for Monitoring a Subway Construction Site. In: W.e.a. Niemeier (Editor), GeoMonitoring 2012. TU Braunschweig, pp. 67–85.
- LAWLEY, R. and GARCIA-BAJO, M., 2009. The National Superficial Deposit Thickness Model (version 5). Information Products Programme. British Geological Survey Internal Report OR/09/049. Available at: http://nora.nerc.ac.uk/8279/1/SDTM_V5_UserGuide.pdf, 18 pp. Accessed on: 07/03/2014.
- LEIGHTON, J.M., SOWTER, A., TRAGHEIM, D., BINGLEY, R.M. and TEFERLE, F.N., 2013. *Land motion in the urban area of Nottingham observed by ENVISAT-1*. International Journal of Remote Sensing, 34(3): 982–1003.
- PAGE, D.P., 1995. *Jubilee Line Extension*. Quarterly Journal of Engineering Geology and Hydrogeology, 28(2): 97–104.
- PIIT, M., 2008. The Pitt review: learning lessons from the 2007 floods, June 2008. Cabinet Office, Met.
- SMITH, A., 2013. Digital Geological Map of Great Britain, information notes, 2013, Nottingham, UK. Available at: <http://nora.nerc.ac.uk/502315/>, 54 pp. Accessed on: 07/03/2014.
- SOWTER, A., BATESON, L., STRANGE, P., AMBROSE, K. and SYAFUDIN, M., 2013. *DInSAR estimation of land motion using intermittent coherence with application to the South Derbyshire and Leicestershire coalfield*. Remote Sensing Letters, 4(10): 979–987.
- STANDING, J.R. and BURLAND, J.B., 2006. *Unexpected tunnelling volume losses in the Westminster area, London*, Géotechnique, pp. 11–26.
- STROZZI, T. and AMBROSI, C., 2007. SAR Interferometric Point Target Analysis and Interpretation of Aerial Photographs for Landslides Investigations in Ticino, Southern Switzerland, ENVISAT Symposium 2007, Montreux, Switzerland.
- SUMBLER, M.A., 1996. British Regional Geology: London and the Thames Valley (4th Edition). London, UK.
- TAPETE, D. and CASAGLI, N., 2013. Testing Computational Methods to Identify Deformation Trends in RADARSAT Persistent Scatterers Time Series for Structural Assessment of Archaeological Heritage. In: B. Murgante, S. Misra, M. Carlini, C. Torre, H.-Q. Nguyen, D. Taniar, B. Apduhan and O. Gervasi (Editors), Computational Science and Its Applications—ICCSA 2013. Lecture Notes in Computer Science. Springer Berlin Heidelberg, pp. 693–707.
- TEATINI, P., STROZZI, T., TOSI, L., WEGMÜLLER, U., WERNER, C. and CARBOGNIN, L., 2007. *Assessing short- and long-time displacements in the Venice coastland by synthetic aperture radar interferometric point target analysis*. Journal of Geophysical Research: Earth Surface, 112(F1): F01012.
- WALSBY, J.C., 2008. Geosure: a bridge between geology and decision making. In: D.G.E. Liverman, C.P.G. Pereira and B. Marker (Editors), Communicating Environmental Geoscience. Geological Society, London, UK, pp. 81–87.
- WEGMULLER, U., WALTER, D., SPRECKELS, V. and WERNER, C., 2010. *Nonuniform Ground Motion Monitoring With TerraSAR-X Persistent Scatterer Interferometry*. Geoscience and Remote Sensing, IEEE Transactions on, 48(2): 895–904.
- WERNER, C., WEGMULLER, U., STROZZI, T. and WIESMANN, A., 2003. Interferometric point target analysis for deformation mapping. 2003 IEEE International Geoscience and Remote Sensing Symposium (IGARSS 2003), vol. 7, pp. 4362–4364.